Connectivity between the visual word form area and the parietal lobe improves after the first year of reading instruction: a longitudinal MRI study in children

Eric Moulton, Florence Bouhali, Karla Monzalvo, Cyril Poupon, Hui Zhang, Stanislas Dehaene, Ghislaine Dehaene-Lambertz, Jessica Dubois

Connectivity between the Visual Word Form Area and the parietal lobe improves after the first year of reading instruction: a longitudinal MRI study in children

Eric Moulton[1,2*], Florence Bouhali[2,3], Karla Monzalvo[1], Cyril Poupon[4], Hui Zhang[5], Stanislas Dehaene[1,6], Ghislaine Dehaene-Lambertz[1], Jessica Dubois[1]

1: Cognitive Neuroimaging Unit U992, INSERM, CEA DRF/Institut-Joliot/NeuroSpin, Université Paris-Saclay, Université Paris-Sud, 91191 Gif/Yvette, France

2: Institut du Cerveau et de la Moelle épinière, ICM, Inserm U 1127, CNRS UMR 7225, Sorbonne Université, F-75013, Paris, France

3: Department of Psychiatry and Weill Institute for Neurosciences, University of California San Francisco (UCSF), San Francisco, CA 94143

4 : UNIRS, CEA DRF/Institut-Joliot/NeuroSpin, Université Paris-Saclay, Université Paris-Sud, 91191 Gif/Yvette, France

5: Department of Computer Science & Centre for Medical Image Computing, University College London, Gower Street, London WC1E 6BT, United Kingdom.

6: Collège de France, Paris, France

***Corresponding author:**
Eric Moulton

E-mail: eric.moulton.jr@gmail.com

Address: Unité INSERM 992 "Neuroimagerie Cognitive"

CEA/SAC/DRF/I2BM/NeuroSpin

Bat 145, point courrier 156

91191 Gif-sur-Yvette, France

March 2019

Abstract

Shortly after reading instruction, a region in the ventral occipital temporal cortex (vOTC) of the left hemisphere, the Visual Word Form Area (VWFA), becomes specialized for written words. Its reproducible location across scripts suggests important anatomical constraints, such as specific patterns of connectivity, notably to spoken language areas. Here, we explored the structural connectivity of the emerging VWFA in terms of its specificity relative to other ventral visual regions and its stability throughout the process of reading instruction in 10 children studied longitudinally over 2 years. Category-specific regions for words, houses, faces, and tools were identified in the left vOTC of each subject with functional MRI. With diffusion MRI and tractography, we reconstructed the connections of these regions at two time points (mean age ± standard deviation: 6.2±0.3, 7.2±0.4 years). We first showed that the regions for each visual category harbor their own specific connectivity, all of which precede reading instruction and remain stable throughout development. The most specific connections of the VWFA were to the dorsal posterior parietal cortex. We then showed that microstructural changes in these connections correlated with improvements in reading scores over the first year of instruction but not one year later in a subsample of 8 children (age: 8.4±0.3 years). These results suggest that the VWFA location depends on its connectivity to distant regions, in particular the left inferior parietal region which may play a crucial role in visual field maps and eye movement dynamics in addition to attentional control in letter-by-letter reading and disambiguation of mirror letters during the first stages of learning to read.

Introduction

The past several decades of functional magnetic resonance imaging (fMRI) research have considerably improved our understanding of the cortical substrates for reading as well as the life-long changes it can induce in the brain (Dehaene et al. 2010b, 2015; Price 2012). Printed words are processed by a largely distributed cortical "reading network", including areas such as the left middle and superior temporal gyri, the left supramarginal gyrus, the left inferior frontal gyrus, posterior parietal cortex, and a region in the left ventral occipitotemporal cortex (vOTC) specialized for recognizing written words termed the Visual Word Form Area (VWFA) (Jobard et al. 2003; McCandliss et al. 2003; Cohen and Dehaene 2004; Dehaene et al. 2015).

The emergence of the VWFA is the result of a culturally acquired skill. Pre-literate children (Monzalvo et al. 2012; Dehaene-Lambertz et al. 2018) and illiterate adults show no specific activity for words in this region (Dehaene et al. 2010b), while preference for words develops at this site after minimal reading instruction (Brem et al. 2010; Lochy et al. 2016; Dehaene-Lambertz et al. 2018). Even literates show a weaker activity for unknown writing and false fonts in this region (Dehaene et al. 2010b). The VWFA develops within a mosaic of regions already specialized in processing various categories of visual stimuli (Grill-Spector and Weiner, 2014; Dehaene-Lambertz et al, 2018) such as houses (Epstein and Kanwisher 1998), faces (Kanwisher et al. 1997), and tools (Grill-Spector et al. 2001), which are already present as early as 5-6 years old (Scherf et al. 2007; Cantlon et al. 2011; Kersey et al. 2015). It is systematically located within the occipitotemporal sulcus (OTS), around tool and face processing areas (Jobard et al. 2003), regardless of one's language and writing system (Bolger et al. 2005; Rueckl et al. 2015).

To explain its highly reproducible location, at least two non-mutually exclusive hypotheses have been proposed, namely the *shape hypothesis* and the *biased connectivity hypothesis* (Hannagan et al. 2015). The former postulates that the location of a visual category processing area is governed by the local circuitry of the vOTC which is intrinsically apt at recognizing the shapes of objects. In line with this idea, a recent study demonstrated that locally scrambled images of objects, faces, and houses elicited similar responses as intact images, alluding to vOTC's fine tuning of statistical properties of visual stimuli rather than semantically meaningful categories (Coggan et al. 2016). On the other hand, the biased connectivity hypothesis states that the location for a given visual category processing area is determined by its white matter connections to distant cortical areas apt at further processing the specific type of visual stimuli at hand. This hypothesis has been supported through diffusion MRI (Saygin et al. 2012; Osher et al. 2015) and functional correlation fMRI studies (Hutchison et al. 2014; Stevens et al. 2015) investigating either the structural or the functional connectivity of regions processing faces, objects, scenes, and bodies in the adult brain. A landmark study showed that the vOTC's structural connectivity in children before they learned to read predicts the future functional location of the VWFA in the same children after 3 years of reading experience (Saygin et al. 2016), thus providing direct support for the biased connectivity hypothesis (Dehaene and Dehaene-Lambertz 2016).

However, the process of learning to read comprises many stages over the course of several years, each of which could leave its own signature in the brain (Stuart and Coltheart 1988). During the first stage, children progressively learn grapheme-phoneme correspondences and assemble sequences of letters in a sequence of sounds by moving their attention, for instance from the left to the right side of the word. This slow, serial process of letter-by-letter reading, which is thought to involve non-language-related regions such as the inferior parietal cortex (Cohen et al. 2008; Dehaene et al. 2010a) lasts until children have accumulated sufficient orthographic knowledge to rely on parallel letter processing (Grainger and Ziegler 2011). More expert readers accelerate their reading by directly accessing the meaning in anterior temporal areas for frequent words or words with an irregular orthography, or through an orthographic-phonetic conversion that encompasses chunks of letters and involves the posterior superior temporal cortex (Dehaene et al. 2005). As reading performances progresses, activity in the VWFA increases and refines (Olulade et al. 2013).

Because reading may involve different cortical regions at different stages of instruction, short-term longitudinal studies could be beneficial by honing in on the individual dynamics of the emerging VWFA and reading network. To this purpose, we followed ten children longitudinally as they progressed throughout the first two year of reading instruction (initially without any formal reading

experience) using functional and diffusion MRI (see (Dehaene-Lambertz et al. 2018) for the functional part). Here, we detailed and compared the white matter connections of areas dedicated to processing words, faces, houses, and tools in order to identify the pathways of each visual category. We aimed to evaluate whether the *emerging* VWFA – with respect to the surrounding visual vOTC areas – harbors early, specific connections to distant cortical areas already present when children begin learning to read. Given the specificity of the VWFA for reading, we hypothesized that only the connections arising specifically from this region would exhibit reading-related maturational changes, as quantified by changes in diffusion tensor imaging (DTI) parameters. In fact, many previous studies have shown ability-related variations of microstructure in children and adults through voxel-by-voxel analyses (Beaulieu et al., 2005; Deutsch et al., 2005) or by isolating anatomically-defined tracts such as the arcuate fasciculus, the inferior fronto-occipital fasciculus, and the inferior longitudinal fasciculus (Niogi and McCandliss 2006; Rollins et al. 2009; Yeatman et al. 2012, 2011; Saygin et al. 2013; Myers et al. 2014; Welcome and Joanisse 2014; Thiebaut de Schotten et al. 2014; Gullick and Booth 2015; Vanderauwera et al. 2015; Broce et al. 2018). As we shall see, our results suggest a crucial role of ventral temporal-to-parietal cortex connections over the first year of learning to read when children need to focus on letter-by-letter reading.

Materials and Methods

1. Subjects and longitudinal design

Ten children (5 females) were recruited in a longitudinal study (Supplementary Table 1). All were right-handed (except for one boy), native French speakers, with no developmental disorders, hearing or visual deficits. Children had an IQ above 80 and followed the normal French academic curriculum, beginning reading instruction around the typical age of 5.5-6.5 years depending on the month in which they were born compared with the start of the school year in September. Informed consent was obtained from all individual participants included in the study. All of the participants' parents gave their written informed consent for the behavioral tests and MRI scanning. An adapted version of the text was read and given to every participant. They all assented verbally and agreed to write their name on the bottom of the written text as a proof of their will to participate in the study. This study was part of the project "Etude multimodale en neuropsychologie et imagerie du développement cérébral et cognitif et de ses relations avec la variabilité génétique" approved on June 16, 2011 by the ethical committee (CPP Kremlin Bicêtre, N˚ 11–008).

a) MRI Evaluation

Participants were evaluated behaviorally and underwent MRI scanning longitudinally at six different visits at equal intervals from the beginning to the end of the first school year of reading instruction (mean delay between first and sixth visit 12.0 ± 1.1 months) in addition to a seventh visit one year later for a subsample of children (N=8, mean delay from sixth to seventh visit 14.5 ± 3.3 months) (Dehaene-Lambertz et al. 2018). Diffusion MRI data, which constitute the focus of this study, were obtained at three time points (TPs) at the first, sixth, and last visits (herein referred to as TP1, TP2, and TP3; mean ages and standard deviations (SD) at TP1: 6.2±0.3y, at TP2: 7.2±0.4y, at TP3: 8.4 ± 0.3y, Fig. 1, Supplementary Table 1), while behavioral and fMRI data were obtained at each visit (Dehaene-Lambertz et al. 2018). All MRI data were acquired on a 3T Siemens Trio machine with a 12-channel head coil.

b) Behavioral Evaluation

Before recruitment, all participants' school teachers attested to the children's inability to read. At all visits, behavioral scores were measured in each participant using a French battery of reading-related tasks (see (Dehaene-Lambertz et al. 2018)). Among these scores, we herein focused on the number of isolated words read under one minute (words/min) as this metric relies on early decoding abilities, can be reliably and objectively measured across children, and is inter-related with other behavioral scores (Dehaene-Lambertz et al. 2018). All children entered the study with little or no ability to read words (mean±sd words/min at TP1: 1.4±2.1, range 0 to 2, except for one child that could read 7). The number of correct words read in 1 minute (LUM) was 33.4 at the end of the first year (range 16 to 54) and 59.25 for a subset of 8 children who returned for the MRI evaluation at the end of the second

year (range 33 to 89), which is within or above the standardized norm at the end of the second year of school, i.e., 36.7 (±15.8) words per minute (Dehaene-Lambertz et al. 2018). (Fig. 1).

2. Preprocessing and analyses of fMRI images for identification of functional peaks

At all visits, T1-weighted (T1w) anatomical and fMRI images were acquired (Dehaene-Lambertz et al. 2018). Here, we only detailed what is relevant to this particular study, namely the identification of functional peaks for each subject and each visual category, since these individual peaks are further used to define selection regions for tractography (see next section). Among the entire set of visual stimuli used in the functional paradigm, we focused on the functional activations in the left hemisphere for houses, faces, words, and tools (and not numbers and bodies) as they form a mosaic of visual categories from the medial to lateral surface at a similar location on the posterior-anterior axis. The functional paradigm consisted in children viewing categories of visual stimuli presented in 6s-blocks, separated by short resting periods with a fixation cross (details are presented in Supplementary Methods and (Dehaene-Lambertz et al. 2018)). To stay attentive, they had to detect a rare target (the picture of a cartoon character "Waldo"). For the current analysis, we only considered the 6 fMRI sessions spanning the first year of reading instruction, for which we had data from the entire child cohort (N=10) sufficient to identify the regions corresponding to the different visual categories ((Dehaene-Lambertz et al. 2018) showed that those regions do not change in location).

At each visit, fMRI images were pre-processed by standard procedures with SPM8 in Matlab (http://www.fil.ion.ucl.ac.uk/spm/) as previously described in (Monzalvo and Dehaene-Lambertz 2013). Functional images were then normalized onto a study-dedicated template in MNI space.

All analyses were performed at the subject level and not the group level. For first-level analyses, brain responses were modeled based on a general linear model using the canonical SPM hemodynamic response function and its time derivative convolved with each experimental condition block. Movement parameters (translation and rotation) were entered as nuisance variables. For words, we hypothesized that VWFA activity would gradually increase with reading experience over the six sessions (Brem et al. 2010; Dehaene et al. 2010b; Eberhard-Moscicka et al. 2015). We therefore constructed "words – other visual stimuli" contrast vectors for each session weighted by the subject's mean-centered reading scores over the six sessions. For houses, faces, and tools, unweighted contrasts "stimuli – other visual stimuli" over all sessions were used. For each child and visual category, we chose the most significant peak (highest T statistic, see Supplementary Methods) consistent with the spatial functional architecture of the ventral temporal cortex (Grill-Spector and Weiner 2014). In this way, from the most medial to lateral, we restrained house peaks to the collateral sulcus for the parahippocampal place area (PPA) (Epstein and Kanwisher 1998), faces to the mid-fusiform face-selective region on the lateral fusiform gyrus (FG4) (Lorenz et al. 2017), words to the occipitotemporal sulcus (OTS) (Reinholz and Pollmann 2005), and tools to the caudal-dorsal subdivision of the lateral occipital cortex (LOC) (Grill-Spector et al. 1999).

3. Individual definition of category-specific pathways with diffusion MRI

a) Image Acquisition and Pre-processing of Diffusion Images

At TP1, TP2, and TP3, diffusion MRI images were acquired with a diffusion-weighted (DW) spin-echo single-shot EPI sequence, with parallel imaging (GRAPPA reduction factor 2) and partial Fourier sampling (factor 6/8). After the acquisition of the b=0s.mm^{-2} volume, diffusion gradients were applied along 45 orientations with b=1000s.mm^{-2}. 48 interleaved axial slices covering the whole brain were acquired with a 2x2x2.5mm^3 spatial resolution (field of view = 256x256mm^2, matrix = 128x128, slice thickness = 2.5mm, TE = 86ms, TR = 9.6s).

Diffusion data were processed using the PTK toolkit and the Connectomist software both developed in-house at NeuroSpin (Duclap et al. 2012). DW images were first corrected for motion artifacts using a dedicated strategy (Dubois et al. 2014b), based on 2 successive steps: (1) automated detection and 2D resampling of slices corrupted by motion or technical problems (e.g., mechanical vibrations and spike noise) and (2) 3D realignment of the 45 diffusion-weighted volumes misregistered due to intervolume motion and distortions stemming from eddy currents. During this procedure, all images were resampled to ensure proper coregistration with anatomical images and to align the anterior

and posterior commissures in an axial plane. The majority of the analyses used diffusion data from TP1 and TP2 as we mainly aimed to study connectivity patterns over the first year of reading instruction, and the number of included subjects was reduced at TP3 (only 8/10 children). This latter time point was only used for microstructural analyses as detailed below in 4.b.

b) Creation of tractography masks and selection regions

At TP1 and TP2, individual tractography masks were constructed from brain segmentations of each subject's anatomical images. To do so, native T1w images were processed with the BrainVISA Morphologist pipeline (Fischer et al. 2012). A white matter segmentation with skeletonized sulci was eroded by 1 voxel to serve as a tractography mask (Guevara et al. 2012). To compute selection regions for tractography, we further identified the superficial white matter by eroding the tractography mask by 1 voxel and considered the subtraction between the eroded tractography mask from the original mask (referred to as the morphological gradient by erosion).

For each child and each visual category, the selection region was generated based on functional peaks in the left hemisphere identified based on fMRI data in the common space as detailed above. Selection regions served to reconstruct the connectivity belonging to the functional patch of cortex for each visual category (see section "Tractography"). A functional peak common across time points was used to ensure that reconstruction of each visual category's connectivity was performed at the same spatial location. After denormalization to native T1w space, each individual functional peak (supposed to be within the cortical sheet) was projected to the closest voxel of the superficial white matter sheet and was geodesically dilated by a 7mm sphere within this sheet in order to respect the 3D geometry of the fusiform territory (Fig. 2a). This choice of dilation radius allowed for maximum coverage of each peak with minimal overlap of two different visual categories (for instance, the closest geodesic distance was on average 16.1mm for words and faces, i.e. more than twice the dilation radius). While we could have used the spatial extent of the fMRI activations to create selection regions for tractography, this would have implied other methodological *a priori* choices, such as the choice of statistical threshold, correction for multiple comparisons, and whether to apply them on the cluster of voxel level, which would still result in a mixture of false positives and negatives. Despite some overlap of the categories of selection regions in T1w space, the next processing step ensured that each selection region covered a unique surface for tractography.

To perfectly overlay the tractography mask and selection regions onto the DW images despite geometric distortions, we matched native T1w images and b=0s.mm^{-2} images for each subject using a non-linear registration method guided by B-splines Free-Form Deformations (Rueckert et al. 1999; Lebenberg et al. 2015). This transformation was applied to the respective tractography masks with a nearest neighbor approximation. In order to regulate the final size of the selection regions, each region was transformed with a cubic interpolation and individually thresholded such that the final selection region would be closest to 30 voxels without any overlap with nearby region for other visual categories (final selection region size ranged from 27 to 36 voxels). Using a repeated-measures ANOVA, we verified that selection region size did not differ significantly between categories ($F(3,27)=1.3, p=0.29$) or time points ($F(1,9)=1.4, p=0.54$; ezANOVA package in R) (Lawrence 2015). With this strategy, we aimed to create localized and specific selection regions that probably reflect the most active patch of cortex of the vOTC for a given visual category.

c) Tractography

To resolve simple crossing fiber configurations, DW images were analyzed based on a fourth order analytical Q-ball model (Descoteaux et al. 2007). Individual 3D tractography was performed with a deterministic algorithm using regularized particle trajectories with an aperture angle of 45° (Perrin et al. 2005; Dubois et al. 2016). Four starting fiber points per voxel of the tractography mask were considered to generate fibers over the whole-brain. For each visual category, we selected streamlines from the whole-brain tractogram that crossed the respective selection region and discarded those that crossed regions of another visual category. The resulting tracts were further converted to 2D maps by counting the number of streamlines per voxel.

4. Group-level analyses of diffusion MRI data

a) Connectivity analyses

To perform group-level analyses across time points and across visual categories, we required a reliable registration technique within and across subjects and opted for DTI-TK (Zhang et al. 2006) which optimizes registration of diffusion tensor data by overlapping corresponding anatomical areas with respect to the orientation of the entire diffusion tensors. This approach has been shown to result in better inter-subject registration in white matter pathways with respect to scalar-based registration strategies such as with FA maps (Wang et al. 2011). Here, we constructed a temporally unbiased population-specific template considering all longitudinal data (TP1, TP2 and TP3) for all children as described in (Keihaninejad et al. 2013), and individual diffusion data were registered onto this template. All voxel-wise analyses were performed in this space. For visualization purposes, we computed the FA map of our study-specific tensor template and registered it to the FMRIB58_FA template using Advanced Normalization Tools (ANTs). We then used the corresponding warp field to project all statistical results in MNI space.

To enable comparisons across the first two time points (TP1 and TP2) for all subjects and categories, individual maps of tracts were (1) warped to this common template, (2) divided by the max value to create density maps (scaled between 0 and 100%), and (3) smoothed with a modest 3mm Gaussian kernel in order to slightly expand the spatial extent of each tract while conserving its specificity, similar to (Bouhali et al. 2014). For each visual category, these subject-level density maps were binarized and averaged over subjects to create a group-level probability map.

The voxel-wise connectivity analyses specified below were performed on the subject-level density maps with FSL's randomise tool (Winkler et al. 2014) using 5000 permutations and the threshold-free cluster enhancement (TFCE) method (Smith and Nichols 2009). In order to avoid statistical differences driven by few subjects, each analysis was restrained to a mask consisting of voxels where the group-level probability for a given visual category was higher than 50% as in (Bouhali et al. 2014). We herein report results significant at a threshold of $p<0.05$, familywise error (FWE) corrected, based on the TFCE statistical image.

The first analysis consisted in evaluating whether category-specific connections changed significantly over the first year of reading instruction. We thus performed a voxel-wise paired t-test comparing the density maps for each visual category at the two time-points (TP1 vs TP2) over the children group, controlling for age and reading scores.

The second analysis consisted in testing the specificity of each visual category's connectivity. Since in previous analysis, we found no significant differences between the two time points for any category-specific connectivity (see Results), we entered density maps of all visual categories from both time points into a repeated-measures analysis of co-variance (ANCOVA) with two within-subject factors (visual category and time point) and two within-subject covariates (age and reading scores). Subjects were treated as a random factor. We tested the specific connectivity of the region for a given visual category against all others (i.e. 3*category-specific density maps – the 3 other maps). The analysis was restrained to the union of masks for all visual categories with group-level probability higher than 50%.

As an additional analysis, we contrasted the face vs word connectivity not only to (1) reproduce previous findings (Bouhali et al. 2014; Saygin et al. 2016), but also to (2) control for a possible bias due to the spatial location of the functional selection regions for tractography. Indeed, the VWFA is located between the faces and tools regions, and its connectivity therefore has two tracts in its immediate vicinity with similar trajectories. On the other hand, the houses and tools regions were respectively the most medial and lateral, and their tracts thus had minimal overlap with other category-specific tracts. These advantageous regions for house and tool categories could have resulted in more tracts captured by many fasciculi of the ventral occipitotemporal cortex. As detailed below, the connectivity specifically related to the VWFA differed depending on the stimuli introduced in the model. Given this model dependency, we aimed to concentrate on the most specific VWFA connectivity that we could identify by controlling for the connections of the other surrounding visual areas. The subsequent microstructure analyses were therefore conducted by considering the results of the analysis with all four visual stimuli.

b) Microstructure analyses

We characterized the microstructure of connections specific to the cortical region processing each visual category with the hypothesis that one's own learning experience can induce white matter changes observable with diffusion MRI (for a review, see (Zatorre et al. 2012)), notably myelin formation or remodeling. Such maturational changes are mostly represented by increases in fractional anisotropy (FA) or decreases in radial diffusivity (RD), two parameters which can be estimated with diffusion tensor imaging (DTI) (Dubois et al. 2014a). Here we also assessed changes in axial diffusivity (AD) to see if correlations were related to a specific direction along the diffusion tensor.

For each child, FA, RD, and AD maps were calculated from the warped tensor images (group space) with DTI-TK functions. For each visual category and each time point, we analyzed the microstructure of the specific tract clusters obtained from the aforementioned voxel-wise ANCOVA. We focused on these group-level category-specific clusters and not on each subject's native connectivity in order to comply with the high overlap between the connectivity of the various visual categories. By restraining our analysis to these clusters, we were able to focus on the microstructural properties of connections for a particular visual category with more specificity and assess if effects observed during the first year generalized to the second year of reading instruction. Within each category-specific cluster, we calculated the average FA, RD, and AD by weighting each voxel by the respective probability of each tract over the children group for each TP. In order to avoid including non-brain or cerebellar regions in the calculation of the average DTI parameters due to spatially smoothing the connectivity maps, we calculated a cerebrum mask by summing and binarizing the entire cortical and subcortical Harvard-Oxford Atlas (with the exception of the brainstem) and back-projected it onto our study specific template. Finally, we computed differences in DTI parameters between TP1 and TP2 as well as between TP2 and TP3.

Regarding statistical analyses, we first evaluated whether DTI parameters changed between each pair of time points using paired t-tests against the null hypothesis over the children group (N=10 for TP1-2, N=8 for TP2-3). We did not compare TP1 and TP3 in order to not lose the temporal dynamics provided by TP2. Second, we evaluated the relationships with improvement in reading scores. We used partial correlations in R software (Kim 2015) to test the relationship between reading improvements and microstructural changes across pairs of time points, all while controlling for the possible confounding effects of increasing age (Adibpour et al. 2018). For each kind of analysis (paired t-test, partial correlation) regarding each DTI parameter, a False Discovery Rate (FDR) correction was applied to correct for multiple comparisons across the four visual categories (statistical threshold for significant relationships: $p_{cor}<0.05$).

Results

1. Connectivity of vOTC category-specific regions

In each child, we identified category-specific regions in the left hemisphere based on functional peaks constrained by anatomical localization. The spatial localization was consistent across children (Supplementary Table 2 describes the individual peak coordinates). Houses were the most medial in the collateral sulcus (mean MNI coordinates x,y,z over the group: -30,-50,-7), followed by faces on the fusiform gyrus (-36,-53,-21), words in the occipitotemporal sulcus (-43,-58,-14), and tools being the most lateral and posterior to words in the occipitotemporal sulcus / posterior inferior temporal gyrus (-41,-70,-10) (Fig. 2a).

In each child, the absolute connectivity for each visual category was visually rather similar (Fig. 2b, Supplementary Figure 1). Tracts showed connections along the ventral occipitotemporal lobe similar to the fibers of the inferior longitudinal fasciculus (ILF) in addition to long-range connections to the inferior prefrontal region likely via the inferior fronto-occopital fasciculus (IFOF) and finally more superior connections to the occipito-parietal junction (Supplementary Figure 1). There was high variability across children in the cortical terminations in more superior regions of the brain (parietal, frontal, pre-frontal) for all categories. However, these variable connections were unaccounted for in the next statistical analyses below which only considered voxels where tracts were present in at least half of the subjects (N=5).

2. Stability of connectivity patterns over the first year of reading instruction

The first voxel-wise ANCOVA with FSL's randomise tool showed that tract topography did not differ significantly between TP1 and TP2 for any visual category (all p_{cor}>0.15), in agreement with the stability of major long-distance connections across development and prior to reading instruction. Changes in age or reading score did not correlate with any difference in connectivity between the two time points (all p_{cor} > 0.12), suggesting that this stable connectivity was not related to inter-individual differences in age or learning ability. In light of this result, we present below the group-level probability maps of each visual category combined over both time points (Fig. 2b).

3. Differences in connectivity patterns between visual categories

Visually, we observed on the group-level probability maps that the most appreciable differences in connectivity across visual categories were for houses, whose tracts densely occupied the inferior medial face of the brain, and for tools, whose tracts were densely connected to the lateral surface (Fig. 2b). The second voxel-wise ANCOVA over TP1 and TP2 quantitatively revealed the specific connectivity for each visual category (Fig. 3), from the most medial to lateral regions. The house region showed strongest connectivity towards the medial surface of the left hemisphere extending from V1 to the anterior portion of the hippocampus. The specific connectivity of the face region was limited to the local ventral temporal surface and showed no long-range connections stronger than for other visual categories. For the VWFA, in addition to strong proximal connections to surrounding cortices, notably the inferior temporal gyrus, we found preferential distal connections to regions extending superiorly and posteriorly to the occipito-parietal junction. Finally, the tool region had the most diffuse connections to the middle and superior temporal gyri, parietal lobe, and the frontal lobe through the external capsule.

Upon restraining the comparison to solely the word and face tracts, the connectivity analysis revealed that the face-specific cluster differed very little from the full analysis including the house and tool tracts (Supplementary Fig. 2). On the contrary, the word-specific cluster occupied a considerably broader area of the ventral surface extending from the occipital to temporal poles. Logically, the parietal connections were still detected. Tracts following the typical trajectory of the arcuate fasciculus were visible, yet in our cohort, less than 50% of subjects had connections reaching the frontal lobe through this pathway. The word-specific cluster also reached up and extended along the middle temporal gyrus (bottom row in Supplementary Fig. 2). Compared to our original analysis, the most striking difference was the frontal terminations of this cluster through the external capsule, which was previously occupied by the tool-specific cluster.

4. Microstructural changes in specific connections related to reading improvement

Lastly, we characterized the changes in microstructural properties of the specific connections for a cortical region processing one visual category over others based on DTI quantification in each cluster. Between TP1 and TP2, only the tool-specific cluster showed a decreasing RD (t= -3.23, p_{cor}=0.041) (Supplementary Table 3). We proceeded to investigate how learning to read might specifically affect microstructural changes over the first year of reading instruction and observed that only the word-specific cluster showed DTI changes related to improvements in reading score, after controlling for age increase (partial correlation between changes in RD and reading scores: r=-0.81, p_{cor}=0.03; same trend for AD: r=-0.74, p_{cor}=0.09) (Fig. 4, Table 1). More precisely, those children who improved in the number of words they could read per minute during the first year of instruction also showed more pronounced decreases in RD in the connections between the VWFA and the occipito-parietal junction, suggesting a specific maturation in relation to fiber myelination during the learning process.

Regarding the second year of learning instruction (analyses between TP2 and TP3 over the same category-specific clusters), we again observed a trending decrease in RD in the tool-specific cluster (t= -3.317, p_{cor}=0.051), and an increasing FA in all clusters except for words (houses: t=4.58, p_{cor}=0.005; faces: t=2.76, p_{cor}=0.038; tools: t=4.71, p_{cor}=0.005) (Supplementary Table 3). Subsequent partial correlations between DTI indices and improvement in reading score, controlling for increase in age, revealed no significant correlations in any category-specific clusters (all p_{cor} > 0.4, Table 1).

Discussion

In this study, we had the rare opportunity to longitudinally evaluate the brain organization in 10 children during the first year of reading instruction as well as a year later in a subgroup of 8 subjects. We were able to reconstruct the specific structural connections of the emerging VWFA in addition to the already present regions processing for houses, faces, and tools, using selection regions for tractography that were functionally defined in individual children. Applying a state-of-the-art registration technique and a statistical approach to compare tracts in a temporally unbiased and reliable manner despite the small sample size, we showed that cortical areas for each visual category revealed a differential set of specific connections. Furthermore, only the word-specific connections to inferior parietal regions exhibited microstructural changes in line with reading improvements over the course of the first year of instruction, but not over the second. We hereby discuss the relevance of these findings in regards to the beginning stages of learning to read.

1. Connectivity of the ventral occipito-temporal cortices

On the whole, the absolute connectivity of the VWFA in children showed similar trajectories as for regions processing houses, faces, and tools, including the inferior longitudinal and fronto-occipital fascicles (ILF and IFOF), and temporoparietal white matter tracts. Only a few subjects had connections from the VWFA extending into either the long or posterior segments of the arcuate fasciculus. Compared with other visual categories, the word-specific connectivity consisted of immediate local connections to the inferior temporal gyrus, and the only long-range connections were those passing superiorly and posteriorly to the occipito-parietal junction and inferior parietal cortex.

Before discussing these results, we first address certain aspects of our methodology. While low statistical power due to the small sample sizes is a known problem in neuroimaging studies on reading in children (Ramus et al. 2018), a landmark study by Saygin et al. (2016), which showed that the VWFA connectivity predates its functional emergence, had a comparable sample size (N=11) as ours (N=10). In fact, our small sample size was partly a compromise for the longitudinal nature of our study, with our child cohort being scanned at 7 different time points and diffusion MRI data acquired at 3 of them. This allowed us to carefully study the early vOTC connectivity and the short-term evolution of its microstructural changes at close intervals. Since our analyses relied on in-sample correlations, our study serves to report and describe – but not predict – changes and their relationships with reading improvements. While recent studies with larger sample sizes have acquired pre- and post-reading instruction imaging data in children (Myers et al. 2014; Vanderauwera et al. 2018), to our knowledge, no study has acquired similar data at such close time points. Nevertheless, the findings we observed between TP2 and TP3 might have been influenced by the lower number of subjects (N=8) than for TP1-TP2 (N=10). For this reason, as well as losing important chronological information, we did not compare TP3 and TP1.

In addition, the resulting word connectivity cluster may have been susceptible to false negatives not only from smoothing but also from controlling for the connectivity of three adjacent functional regions. While our b-value of 1000s.mm^{-2} could be considered low for resolving crossing fibers, it is comparable to that used in related studies so far (Saygin et al. 2016; Broce et al. 2018). Here, it cannot be ruled out that future studies at higher b-values will allow researchers to highlight subtle differences in reading connectivity throughout development. Despite these drawbacks, other aspects of our methodology were carefully considered to ensure the robustness of the findings. First, we acquired 45 DW images in non-collinear directions and used a specific strategy to correct for motion artifacts that allowed us to not discard any data. Given the limited amount of scanning time available in young children, this type of acquisition probably approaches the maximum of what is reasonably feasible. Second, to register data over the children group, we employed DTI-TK, an optimal technique demonstrated to better align white matter structures than other software (Wang et al. 2011). Finally, our definition of selection regions for tractography was tailored to each subject's functional peaks and local cortical morphology, and we investigated the connectivity of several functional areas, more than what has usually been done.

The most similar study to ours was conducted by (Saygin et al. 2016) who scanned children before and three years after the beginning of reading instruction with diffusion MRI and fMRI, focusing

on the cortical terminations of tracts. They were able to show that the cortical connectivity from vOTC seeds at the pre-reading time point (~5 years of age) predicted the functional location of the VWFA within the vOTC three years later. Here, we further studied the microstructural changes in the specific white matter connections for each visual category and related these changes to age and reading improvement. In particular, we showed not only that the VWFA in children has early, specific connections with respect to the surrounding cortex but also that they mature in response to reading instruction.

The biased-connectivity hypothesis (Hannagan et al. 2015) suggests that predominant direct connections to language areas, such as the superior temporal gyrus or the inferior frontal gyrus, would explain the consistent location of the VWFA in adults and throughout the process of learning to read. VWFA did project to some of these regions (Fig. 2). However, we did not find evidence that these connections were unique to VWFA. The most prominent word-specific connections in our children cohort terminated in parietal cortex, and conversely, it was the connections originating from the tools region in the lateral occipital cortex which had the most projections to frontal and temporal language areas.

At first sight, these results might seem surprising, as other studies have suggested that the VWFA does indeed harbor connections to language areas in adults and 7-11yo children (Epelbaum et al. 2008; Yeatman et al. 2011; Bouhali et al. 2014). In fact, there might be different non-exclusive explanations for this apparent discrepancy. First, we considered four selection regions for tractography that were relatively close along the cortical surface, so reconstructed tracts had some spatial vicinity with each other. This might be problematic for tracts originating from the middle regions (i.e., for faces and words), since the possible overlap was related to two neighboring tracts rather than one for tracts from the external regions (i.e., for houses and tools). When we re-ran the same statistical analysis keeping solely the face and word connections as in previous studies (Bouhali et al. 2014; Stevens et al. 2017) and removing the tool and house connections, we observed a much more diffuse cluster for words-specific connections (including the previously reported parietal connections but also more ventral projections from the occipital to temporal poles in addition to and long-range connections to the inferior frontal lobe through the external capsule) (see Supplementary Fig. 2), while that for faces remained virtually unchanged. The face connectivity likely did not change as it was already rather separate from the house peaks along the lateral-medial axis, whereas for words and tools, their respective locations were much closer (see Supplementary Table 2). Results on the word-specific connectivity thus strongly differed depending on the neighboring tracts that are considered in the statistical analysis. Consequently, it remains difficult to compare our findings obtained using four visual category areas with previous studies that only investigated the connectivity of two areas at once.

Regarding the location of the selection region for words, it is interesting to note that the adult VWFA takes part in a posterior-anterior functional gradient of word-sensitive areas, going from posterior regions sensitive to certain line arrangements to anterior regions preferentially responding to the most frequent recurring substrings and small words in one's learned script (Dehaene et al. 2005; Baker et al. 2007; Vinckier et al. 2007; Chan et al. 2009; Seghier and Price 2011). Anatomical connectivity reflects this posterior-anterior gradient, as the connectivity with oral language regions increases from posterior to anterior regions (Fan et al. 2014; Bouhali et al. 2014). A roughly similar functional gradient is visible in children (van der Mark et al. 2009; Monzalvo et al. 2012) even if it is less differentiated than in adults (Olulade et al. 2013), suggesting that functional specificity gradually develops along years of reading instruction and practice. However, the average coordinate that we identified in children ([-43.2mm, -58.0mm, -14.0mm] in MNI-space) is very close to the adult VWFA ([-42mm, 57mm, -15mm] in (Cohen et al. 2002)), and the individual peaks remained at the same location during the two first years of reading instruction (Dehaene-Lambertz et al. 2018), suggesting that tractography was performed from similar regions as in other studies.

Because these children were followed longitudinally during two years, it was possible to retrospectively examine the response of the VWFA voxels before they learned to read. These voxels were weakly but steadily selective to the tools category (Dehaene-Lambertz et al. 2018). This functional overlap, together with limits in scanning resolution and inter-subject averaging might explain why the word and tool regions appears to share overlapping connectivity in the present study.

Furthermore, since tractography performance depends on the fibers' anisotropy and myelination, one might expect to detect connections that are maturing more intensely than neighboring fibers. Here, we might have highlighted the specific connections to the parietal lobe given that parietal regions are particularly recruited during the first stage of reading, to decode words on a letter-by-letter basis (Grainger and Ziegler 2011). At a later, more automatized stage (i.e. in older children) when faster access to word meaning is reached, connections with language areas might become easier to tract due to increased myelination.

2. Parietal projections of the VWFA

The parietal lobe is a complex associative cortex involved in a plethora of higher cognitive functions including mental subtraction, saccades, finger pointing, grasping, as well as converting orthography to phonology and to semantics (Simon et al. 2002; Vigneau et al. 2006). Most notably, the parietal cortex is implicated in the control of visual attention (Vidyasagar 1999; Saalmann et al. 2007). This type of control is essential during the first stage of reading (Vidyasagar 1999; Pammer et al. 2006; Grainger and Ziegler 2011) when children learn to direct their attention from left to right and top to bottom along the page (in occidental languages) and to disambiguate mirror-letters such as "b" and "d" (Dehaene et al. 2010a).

So far, several fMRI studies have observed co-activation of the parietal lobes with the VWFA in many circumstances. Adults recruit it during serial effortful reading of words that are distorted through rotation, increased letter spacing, hemifield shifting, or low contrast (Cohen et al. 2008; Rosazza et al. 2009; Kay and Yeatman 2017). Moreover, the increased activation of the parietal lobes in viewing such distorted words is accompanied by more posterior activity of the VWFA than when viewing words in their normal format (Cohen et al. 2008), perhaps due to the ventral-to-dorsal connections of this area (Yeatman et al. 2014). These studies suggest that when the automatic parallel processing of bigrams cannot be performed, subjects revert to letter-by-letter reading, thus relying more on early level word processing and attentional control involving the parietal cortex. As an illustration, one reported patient who had bilateral occipito-parietal atrophy with an intact vOTC was unable to read words presented vertically, words with double-spaced letters, or words in mirror-reversed form; however, reading words in their normal, horizontal form was preserved (Vinckier et al. 2006). Strong attention to normally presented words and consonant strings can also elicit activity of the dorsal visual stream in the occipito-parietal junction and intraparietal sulcus (IPS) (Cohen et al. 2003; Cattinelli et al. 2013). The activity of the inferior IPS might also reflect top-down modulations on the VWFA directly related to task demands on word recognition (Kay and Yeatman 2017) or the need to encode letter position (Ossmy et al. 2014).

Altogether, these studies suggest that a major role of the parietal lobe in reading is to focus attentional control on novel or unusual presentations of visual words. Behaviorally, this activity is predominantly reflected in letter-by-letter reading, increasing the reading time with word length (Cohen et al. 2008), an effect that progressively disappears when reading becomes more automatized (Zoccolotti et al. 2005). Because of their lack of expertise and automaticity in word recognition, children may particularly recruit this pathway at the onset of reading acquisition. Indeed, the analyses of our children's functional responses throughout the first year of reading acquisition revealed transitory parietal activation in response to words that disappeared after two years (Dehaene-Lambertz et al. 2018). The present results indicate that, during the same time period, myelination of the connections between VWFA and parietal cortex changed. This observation is also congruent with a comparison done between illiterate and ex-illiterate adults, which found that literacy enhanced the density of gray matter in dorsal occipito-parietal regions (Carreiras et al. 2009). The authors also attribute an important role to the dorsal stream at the beginning stages of reading.

However, beyond attentional mechanisms, eye movement dynamics could also have played a role in driving the observed microstructural changes. A recent study showed that, when reading, children exhibit stereotypical eye movement patterns related to the cortical locations for visual field coverage, which are not the same for adults (Gomez et al. 2018). In children, word-sensitive regions of the vOTC are not located on patches of cortex centered on the fovea, but are slightly eccentric; therefore, they naturally view words slightly off-center such that cortical visual field coverage falls on the center of the word. On the other hand, cortical activity for words in adults is shifted towards the fovea, causing them to place their gaze on the center of words. Since the intraparietal sulcus harbors visual field maps

involved in eye movements (Levy et al. 2007), is also connected to the VWFA, and modulates its activity in relation to task difficulty (Kay and Yeatman 2017), the microstructural changes in connectivity between the VWFA and parietal cortex may also be the result of eye movement dynamics that occur in reading children.

These connections might coincide with (Yeatman et al. 2014)'s description of the vertical occipital fasciculus (VOF), which has recently been proposed to participate in the circuitry of the VWFA (Wandell and Yeatman 2013). The VOF is posited to relay ventral word-shape recognition systems and dorsal visual systems and lesions to this fasciculus can result in pure alexia (Greenblatt 1976). Its most anterior boundary is near the midpoint of the mid-fusiform sulcus (Yeatman et al. 2014; Takemura et al. 2015) and also behind the cortical projections of the posterior arcuate fasciculus (Weiner et al. 2016). It projects superiorly lateral to the IFOF and ILF and terminates in the lateral occipital, inferior parietal lobe, or both. In our case, the more significantly prominent tracts belonging to the VWFA connections projected all the way up to the inferior intraparietal sulcus and the lateral occipito-parietal junction. A study found that the VOF reconstructed with diffusion tractography did indeed connect the intraparietal sulcus to functional peaks of the VWFA in 8 out of 9 adults (Kay and Yeatman 2017). In our cohort, we found that this pathway was also present in the majority of our children (N=7). Our findings suggest that the VOF might play a crucial role in the early reading stage. This idea was recently corroborated by a complementary cross-sectional study in children, which analyzed changes in dissected tracts of the reading network (Broce et al. 2018).

3. Microstructural changes in the word-specific connections with learning to read

As for the specific connectivity between the emerging VWFA and the inferior parietal lobe, predating reading instruction, we showed that an increase in reading ability over the first year of learning correlated with a decrease in radial diffusivity (RD) in only these connections and independently from age increase. Decreasing RD may be indicative of fiber organization, increased myelination, myelin remodeling, astrocyte changes, or angiogenesis (Dubois et al. 2014a), notably when learning a new skill (Zatorre et al. 2012) or increasing the speed of neural information as suggested for visual processing in infants (Dubois et al. 2008; Adibpour et al. 2018). In our child cohort, it thus seems that the connections between the word-specific vOTC and the parietal cortex are involved in the learning process and are mediating crucial information during the first stages of learning to read, which leads to their specific myelination. Interestingly, we observed no correlation in terms of fractional anisotropy; however, this may be explained by the fact that the VOF is a thin fascicle crossed by many fibers (Yeatman et al. 2014; Takemura et al. 2015), which complicates the interpretation of FA compared with RD changes when some pools of crossing fibers become myelinated (Dubois et al. 2014a). Most importantly, no DTI changes in any other category-specific connectivity correlated with the improvement in reading scores, which further reinforced the myelination specificity for word-specific tracts. In fact, isolating the specificity of each visual category's connectivity was necessary to observe these domain-specific maturational changes. In a post-hoc analysis, we used the non-constrained global connectivity maps (shown in Supplementary Figure 1) to perform the same correlation analysis. As expected, global changes in diffusion parameters were not able to reflect reading-related improvements (all $p_{cor}>0.29$, Supplementary Table 4), which remained unique to the word-specific connectivity.

It seems that this reading-related maturation of these connections was also specific to the first year of learning, as we did not observe similar relationships between RD decrease and reading score in the same region over the second year of instruction, but these findings only relied on a sub-group of eight children. Moreover, the variability of changes in diffusion parameters was rather large across children which, combined with the small sample size, could have possibly masked certain effects (Supplementary Table 3).

The corpus of diffusion MRI studies related to reading is abundant, yet, to our knowledge, we are the first team to report changes in vOTC-to-parietal fibers with reading improvements. We provide different explanations as to why no such relationships have heretofore been reported. First, many previous studies relied on ROI-based investigations in which this white matter region was not considered (Rollins et al. 2009; Cui et al. 2016) or used tractography to delineate other white matter bundles (Lebel and Beaulieu 2011; Vandermosten et al. 2012; Saygin et al. 2013; Gullick and Booth 2015; Vanderauwera et al. 2015). Second, for whole-brain voxel-based investigations that could have

identified local correlations in the vOTC-to-parietal white matter region, most of the studies recruited children well after they were able to read (Beaulieu et al. 2005; Deutsch et al. 2005; Odegard et al. 2009; Rimrodt et al. 2010). For the few longitudinal studies with larger sample sizes that acquired baseline data prior to reading instruction, the follow-up scans also fell several years after the first year of learning to read (Schmithorst et al. 2005; Myers et al. 2014; Saygin et al. 2016; Vanderauwera et al. 2018), making it difficult to capture short term consequences of this learning mechanism. One recent study, however, reported relations between diffusion metrics of the VOF in both hemispheres and phonological awareness in a cross-sectional study of 20 children aged 5-8 years old (Broce et al. 2018). The authors mentioned potential involvement of the right hemisphere in early literacy but suggested that activity might shift to the left hemisphere. Our observed correlations between early microstructural changes of the left vOTC-to-parietal white matter and reading improvements support this hypothesis.

We here propose that the vOTC-to-parietal connections are maximally relevant at the beginning stages of learning literacy and would therefore exhibit specific, maturational signatures during this short time frame, and not later on. Whereas the intense myelination of the vOTC-to-parietal connections is specifically related to reading improvement during the first year of instruction, these connections might be less solicited during the second year as reading becomes less effortful. Indeed, as children grow older and improve their reading skills, whole-word reading becomes automatic and goes beyond letter-by-letter decoding. Children would therefore gradually rely less on parietal resources and more on anterior portions of the VWFA territory directly connected to language areas, possibly via the IFOF and AF. Nevertheless, these results should be validated in a larger cohort due to the relative small sample size of the present study.

Conclusion

We reported that the early vOTC connectivity predates reading instruction and already demonstrates specificity to visual categories in 6-year-old children. For words, this specific connectivity involves white matter fibers to the dorsal posterior parietal cortex, and their myelination is uniquely related to reading improvement during the first year of instruction. These findings support children's transient reliance on the parietal lobe for attentional control over novel words and letter-by-letter reading in addition to possible visual field map and eye-movement dynamics during the first stages of learning to read. The role of these connections is likely maximal at the onset of learning when parietal resources are highly solicited to manage the strong attentional demands of effortful grapheme-phoneme decoding. Future studies should reproduce these findings in a larger cohort of children in a longitudinal follow-up with possibly more time points throughout the first year of reading and years beyond. It would then be conceivable to follow the evolution of the VWFA location and its connectivity until the adult stage. In addition, the vOTC-to-parietal connectivity's role in decoding novel words and symbols might be investigated in proficiently reading adults that would be trained to automatize reading in unfamiliar formats, such as vertically. This would constitute a reliable study to control for confounding effects observed with young children such as brain maturation and inter-individual variability in attentional control. We would expect that sufficient training in adults would involve specific microstructural changes in the vOTC-to-parietal white matter as a function of reading ability.

Acknowledgments

The authors would like to thank all the children and their parents who participated in this study, as well as the medical team of UNIACT at Neurospin for precious help in scanning the children, especially Gaëlle Mediouni. We are also grateful to Jessica Lebenberg and Francois Leroy for their help in MRI analyses, to Michel Thiebaut de Schotten and Thomas Hannagan for helpful discussion on this study.

Compliance with Ethical Standards

Funding: This research was supported by a grant from the Fondation Bettencourt-Schueller.

Informed Consent: Informed consent was obtained from all individual participants included in the study.

Ethical approval: All participants and parents gave their written informed consent for the behavioral

tests and MRI scanning, and the study was approved by the local ethics committee for biomedical research.

Conflict of Interest: The authors declare that they have no conflict of interest.

References

Adibpour P, Dubois J, Dehaene-Lambertz G (2018) Right but not left hemispheric discrimination of faces in infancy. Nat Hum Behav 2:67–79. doi: 10.1038/s41562-017-0249-4

Baker CI, Liu J, Wald LL, et al (2007) Visual word processing and experiential origins of functional selectivity in human extrastriate cortex. Proc Natl Acad Sci 104:9087–9092. doi: 10.1073/pnas.0703300104

Beaulieu C, Plewes C, Paulson LA, et al (2005) Imaging brain connectivity in children with diverse reading ability. Neuroimage 25:1266–71. doi: 10.1016/j.neuroimage.2004.12.053

Bolger DJ, Perfetti CA, Schneider W (2005) Cross-cultural effect on the brain revisited: Universal structures plus writing system variation. Hum Brain Mapp 25:92–104. doi: 10.1002/hbm.20124

Bouhali F, Thiebaut de Schotten M, Pinel P, et al (2014) Anatomical Connections of the Visual Word Form Area. J Neurosci 34:15402–15414. doi: 10.1523/JNEUROSCI.4918-13.2014

Brem S, Bach S, Kucian K, et al (2010) Brain sensitivity to print emerges when children learn letter-speech sound correspondences. Proc Natl Acad Sci U S A 107:7939–44. doi: 10.1073/pnas.0904402107

Broce IJ, Bernal B, Altman N, et al (2018) Fiber pathways supporting early literacy development in 5–8-year-old children. Brain Cogn 1–10. doi: 10.1016/j.bandc.2018.12.004

Cantlon JF, Pinel P, Dehaene S, Pelphrey KA (2011) Cortical representations of symbols, objects, and faces are pruned back during early childhood. Cereb Cortex 21:191–199. doi: 10.1093/cercor/bhq078

Carreiras M, Seghier ML, Baquero S, et al (2009) An anatomical signature for literacy. Nature 461:983–986. doi: 10.1038/nature08461

Cattinelli I, Borghese NA, Gallucci M, Paulesu E (2013) Reading the reading brain: A new meta-analysis of functional imaging data on reading. J Neurolinguistics 26:214–238. doi: 10.1016/j.jneuroling.2012.08.001

Chan S tak, Tang S wing, Tang K wing, et al (2009) Hierarchical coding of characters in the ventral and dorsal visual streams of Chinese language processing. Neuroimage 48:423–435. doi: 10.1016/j.neuroimage.2009.06.078

Coggan DD, Liu W, Baker DH, Andrews TJ (2016) Category-selective patterns of neural response in the ventral visual pathway in the absence of categorical information. Neuroimage 135:107–114. doi: 10.1167/15.12.622

Cohen L, Dehaene S (2004) Specialization within the ventral stream: The case for the visual word form area. Neuroimage 22:466–476. doi: 10.1016/j.neuroimage.2003.12.049

Cohen L, Dehaene S, Vinckier F, et al (2008) Reading normal and degraded words: Contribution of the dorsal and ventral visual pathways. Neuroimage 40:353–366. doi: 10.1016/j.neuroimage.2007.11.036

Cohen L, Lehéricy S, Chochon F, et al (2002) Language-specific tuning of visual cortex? Functional properties of the Visual Word Form Area. Brain 125:1054–69. doi: 10.1093/brain/awf094

Cohen L, Martinaud O, Lemer C, et al (2003) Visual Word Recognition in the Left and Right Hemispheres: Anatomical and Functional Correlates of Peripheral Alexias. Cereb Cortex 13:1313–1333. doi: 10.1093/cercor/bhg079

Cui Z, Xia Z, Su M, et al (2016) Disrupted white matter connectivity underlying developmental dyslexia: A machine learning approach. Hum Brain Mapp 37:1443–1458. doi: 10.1002/hbm.23112

Dehaene-Lambertz G, Monzalvo K, Dehaene S (2018) The emergence of the visual word form: Longitudinal evolution of category-specific ventral visual areas during reading acquisition. PLOS Biol 16:e2004103. doi: 10.1371/journal.pbio.2004103

Dehaene S, Cohen L, Morais J, Kolinsky R (2015) Illiterate to literate: behavioural and cerebral changes induced by reading acquisition. Nat Rev Neurosci 16:234–44. doi: 10.1038/nrn3924

Dehaene S, Cohen L, Sigman M, Vinckier F (2005) The neural code for written words: A proposal. Trends Cogn Sci 9:335–341. doi: 10.1016/j.tics.2005.05.004

Dehaene S, Dehaene-Lambertz G (2016) Is the brain prewired for letters? Nat Neurosci 19:1192–3. doi: 10.1038/nn.4369

Dehaene S, Nakamura K, Jobert A, et al (2010a) Why do children make mirror errors in reading? Neural correlates of mirror invariance in the visual word form area. Neuroimage 49:1837–48. doi:

10.1016/j.neuroimage.2009.09.024

Dehaene S, Pegado F, Braga LW, et al (2010b) How learning to read changes the cortical networks for vision and language. Science 330:1359–64. doi: 10.1126/science.1194140

Descoteaux M, Angelino E, Fitzgibbons S, Deriche R (2007) Regularized, fast, and robust analytical Q-ball imaging. Magn Reson Med 58:497–510. doi: 10.1002/mrm.21277

Deutsch GK, Dougherty RF, Bammer R, et al (2005) Children's reading performance is correlated with white matter structure measured by diffusion tensor imaging. Cortex 41:354–63

Dubois J, Dehaene-Lambertz G, Kulikova S, et al (2014a) The early development of brain white matter: a review of imaging studies in fetuses, newborns and infants. Neuroscience 276:48–71. doi: 10.1016/j.neuroscience.2013.12.044

Dubois J, Dehaene-Lambertz G, Soares C, et al (2008) Microstructural Correlates of Infant Functional Development: Example of the Visual Pathways. J Neurosci 28:1943–1948. doi: 10.1523/JNEUROSCI.5145-07.2008

Dubois J, Kulikova S, Hertz-Pannier L, et al (2014b) Correction strategy for diffusion-weighted images corrupted with motion: Application to the DTI evaluation of infants' white matter. Magn Reson Imaging 32:981–992. doi: 10.1016/j.mri.2014.05.007

Dubois J, Poupon C, Thirion B, et al (2016) Exploring the Early Organization and Maturation of Linguistic Pathways in the Human Infant Brain. Cereb Cortex 26:2283–2298. doi: 10.1093/cercor/bhv082

Duclap D, Schmitt B, Lebois A, et al (2012) Connectomist-2.0: a novel diffusion analysis toolbox for BrainVISA. In: Proceedings of the 29th ESMRMB meeting

Eberhard-Moscicka AK, Jost LB, Raith M, Maurer U (2015) Neurocognitive mechanisms of learning to read: Print tuning in beginning readers related to word-reading fluency and semantics but not phonology. Dev Sci 18:106–118. doi: 10.1111/desc.12189

Epelbaum S, Pinel P, Gaillard R, et al (2008) Pure alexia as a disconnection syndrome: new diffusion imaging evidence for an old concept. Cortex 44:962–74. doi: 10.1016/j.cortex.2008.05.003

Epstein R, Kanwisher N (1998) A cortical representation of the local visual environment. Nature 392:598–601. doi: 10.1038/33402

Fan Q, Anderson AW, Davis N, Cutting LE (2014) Structural connectivity patterns associated with the putative visual word form area and childrens reading ability. Brain Res 1586:118–129. doi: 10.1016/j.brainres.2014.08.050

Fischer C, Operto G, Laguitton S, et al (2012) Morphologist 2012: the new morphological pipeline of BrainVISA. In: Proceedings of the 18th HBM Scientific Meeting, Beijing, China. NeuroImage. p 670

Gomez J, Natu V, Jeska B, et al (2018) Development differentially sculpts receptive fields across early and high-level human visual cortex. Nat Commun 9:. doi: 10.1038/s41467-018-03166-3

Grainger J, Ziegler JC (2011) A dual-route approach to orthographic processing. Front Psychol 2:1–13. doi: 10.3389/fpsyg.2011.00054

Greenblatt SH (1976) Subangular alexia without agraphia or hemianopsia. Brain Lang 3:229–245. doi: 10.1016/0093-934X(76)90019-5

Grill-Spector K, Kourtzi Z, Kanwisher N (2001) The lateral occipital complex and its role in object recognition. Vision Res 41:1409–1422. doi: 10.1016/S0042-6989(01)00073-6

Grill-Spector K, Kushnir T, Edelman S, et al (1999) Differential processing of objects under various viewing conditions in the human lateral occipital complex. Neuron 24:187–203. doi: 10.1016/S0896-6273(00)80832-6

Grill-Spector K, Weiner KS (2014) The functional architecture of the ventral temporal cortex and its role in categorization. Nat Rev Neurosci 15:536–548. doi: 10.1038/nrn3747

Guevara P, Duclap D, Poupon C, et al (2012) Automatic fiber bundle segmentation in massive tractography datasets using a multi-subject bundle atlas. Neuroimage 61:1083–99. doi: 10.1016/j.neuroimage.2012.02.071

Gullick MM, Booth JR (2015) The direct segment of the arcuate fasciculus is predictive of longitudinal reading change. Dev Cogn Neurosci 13:68–74. doi: 10.1016/j.dcn.2015.05.002

Hannagan T, Amedi A, Cohen L, et al (2015) Origins of the specialization for letters and numbers in ventral occipitotemporal cortex. Trends Cogn Sci 19:374–382. doi: 10.1016/j.tics.2015.05.006

Hutchison RM, Culham JC, Everling S, et al (2014) Distinct and distributed functional connectivity patterns across cortex reflect the domain-specific constraints of object, face, scene, body, and tool category-selective modules in the ventral visual pathway. Neuroimage 96:216–36. doi: 10.1016/j.neuroimage.2014.03.068

Jobard G, Crivello F, Tzourio-Mazoyer N (2003) Evaluation of the dual route theory of reading: A metanalysis of 35 neuroimaging studies. Neuroimage 20:693–712. doi: 10.1016/S1053-8119(03)00343-4

Kanwisher N, McDermott J, Chun MM (1997) The fusiform face area: a module in human extrastriate cortex specialized for face perception. J Neurosci 17:4302–11. doi: 10.1098/Rstb.2006.1934

Kay KN, Yeatman JD (2017) Bottom-up and top-down computations in word- and face-selective cortex. Elife 6:35–47. doi: 10.7554/eLife.22341

Keihaninejad S, Zhang H, Ryan NS, et al (2013) An unbiased longitudinal analysis framework for tracking white matter changes using diffusion tensor imaging with application to Alzheimer's disease. Neuroimage 72:153–163. doi: 10.1016/j.neuroimage.2013.01.044

Kersey AJ, Clark TS, Lussier C a., et al (2015) Development of Tool Representations in the Dorsal and Ventral Visual Object Processing Pathways. Cereb Cortex 1–11. doi: 10.1093/cercor/bhv140

Kim S (2015) ppcor: An R Package for a Fast Calculation to Semi-partial Correlation Coefficients. Commun Stat Appl methods 22:665–674. doi: 10.5351/CSAM.2015.22.6.665

Lawrence MA (2015) ez: Easy Analysis and Visualization of Factorial Experiments. R package version 4.3

Lebel C, Beaulieu C (2011) Longitudinal development of human brain wiring continues from childhood into adulthood. J Neurosci 31:10937–47. doi: 10.1523/JNEUROSCI.5302-10.2011

Lebenberg J, Poupon C, Thirion B, et al (2015) Clustering the infant brain tissues based on microstructural properties and maturation assessment using multi-parametric MRI. In: ISBI

Levy I, Schluppeck D, Heeger DJ, Glimcher PW (2007) Specificity of human cortical areas for reaches and saccades. J Neurosci 27:4687–96. doi: 10.1523/JNEUROSCI.0459-07.2007

Lochy A, Van Reybroeck M, Rossion B (2016) Left cortical specialization for visual letter strings predicts rudimentary knowledge of letter-sound association in preschoolers. Proc Natl Acad Sci 113:8544–8549. doi: 10.1073/pnas.1520366113

Lorenz S, Weiner KS, Caspers J, et al (2017) Two New Cytoarchitectonic Areas on the Human Mid-Fusiform Gyrus. Cereb Cortex 27:373–385. doi: 10.1093/cercor/bhv225

McCandliss BD, Cohen L, Dehaene S (2003) The visual word form area: Expertise for reading in the fusiform gyrus. Trends Cogn Sci 7:293–299. doi: 10.1016/S1364-6613(03)00134-7

Monzalvo K, Dehaene-Lambertz G (2013) How reading acquisition changes children's spoken language network. Brain Lang 127:356–365. doi: 10.1016/j.bandl.2013.10.009

Monzalvo K, Fluss J, Billard C, et al (2012) Cortical networks for vision and language in dyslexic and normal children of variable socio-economic status. Neuroimage 61:258–274. doi: 10.1016/j.neuroimage.2012.02.035

Myers CA, Vandermosten M, Farris EA, et al (2014) Structural changes in white matter are uniquely related to children's reading development. Psychol Sci 25:1870–1883. doi: 10.1177/0956797614544511

Niogi SN, McCandliss BD (2006) Left lateralized white matter microstructure accounts for individual differences in reading ability and disability. Neuropsychologia 44:2178–88. doi: 10.1016/j.neuropsychologia.2006.01.011

Odegard TN, Farris EA, Ring J, et al (2009) Brain connectivity in non-reading impaired children and children diagnosed with developmental dyslexia. Neuropsychologia 47:1972–1977. doi: 10.1016/j.neuropsychologia.2009.03.009

Olulade OA, Flowers DL, Napoliello EM, Eden GF (2013) Developmental differences for word processing in the ventral stream. Brain Lang 125:134–145. doi: 10.1016/j.bandl.2012.04.003

Osher DE, Saxe RR, Koldewyn K, et al (2015) Structural Connectivity Fingerprints Predict Cortical Selectivity for Multiple Visual Categories across Cortex. Cereb Cortex bhu303-. doi: 10.1093/cercor/bhu303

Ossmy O, Ben-Shachar M, Mukamel R (2014) Decoding letter position in word reading. Cortex 59:74–83. doi: 10.1016/j.cortex.2014.07.002

Pammer K, Hansen P, Holliday I, Cornelissen P (2006) Attentional shifting and the role of the dorsal pathway in visual word recognition. Neuropsychologia 44:2926–2936. doi: 10.1016/j.neuropsychologia.2006.06.028

Perrin M, Poupon C, Cointepas Y, et al (2005) Fiber tracking in q-ball fields using regularized particle trajectories.

Inf Process Med Imaging 19:52–63

Price CJ (2012) A review and synthesis of the first 20years of PET and fMRI studies of heard speech, spoken language and reading. Neuroimage 62:816–847. doi: 10.1016/j.neuroimage.2012.04.062

Ramus F, Altarelli I, Jednoróg K, et al (2018) Neuroanatomy of developmental dyslexia: Pitfalls and promise. Neurosci. Biobehav. Rev. 84:434–452

Reinholz J, Pollmann S (2005) Differential activation of object-selective visual areas by passive viewing of pictures and words. Cogn Brain Res 24:702–714. doi: 10.1016/j.cogbrainres.2005.04.009

Rimrodt SL, Peterson DJ, Denckla MB, et al (2010) White matter microstructural differences linked to left perisylvian language network in children with dyslexia. Cortex 46:739–749. doi: 10.1016/j.cortex.2009.07.008

Rollins NK, Pickering J, Hughes CW (2009) in Children : Alterations in Diffusion- Tensor Metrics of White Matter Tracts Purpose : Methods : Results : Conclusion : 251:

Rosazza C, Cai Q, Minati L, et al (2009) Early involvement of dorsal and ventral pathways in visual word recognition: An ERP study. Brain Res 1272:32–44. doi: 10.1016/j.brainres.2009.03.033

Rueckert D, Sonoda LI, Hayes C, et al (1999) Nonrigid registration using free-form deformations: application to breast MR images. IEEE Trans Med Imaging 18:712–21. doi: 10.1109/42.796284

Rueckl JG, Paz-Alonso PM, Molfese PJ, et al (2015) Universal brain signature of proficient reading: Evidence from four contrasting languages. Proc Natl Acad Sci 112:15510–15515. doi: 10.1073/pnas.1509321112

Saalmann YB, Pigarev IN, Vidyasagar TR (2007) Neural Mechanisms of Visual Attention: How Top-Down Feedback Highlights Relevant Locations. Science (80-) 316:1612–1615. doi: 10.1126/science.1139140

Saygin ZM, Norton ES, Osher DE, et al (2013) Tracking the roots of reading ability: white matter volume and integrity correlate with phonological awareness in prereading and early-reading kindergarten children. J Neurosci 33:13251–8. doi: 10.1523/JNEUROSCI.4383-12.2013

Saygin ZM, Osher DE, Koldewyn K, et al (2012) Anatomical connectivity patterns predict face selectivity in the fusiform gyrus. Nat Neurosci 15:321–7. doi: 10.1038/nn.3001

Saygin ZM, Osher DE, Norton ES, et al (2016) Connectivity precedes function in the development of the visual word form area. Nat Neurosci 19:1250–5. doi: 10.1038/nn.4354

Scherf KS, Behrmann M, Humphreys K, Luna B (2007) Visual category-selectivity for faces, places and objects emerges along different developmental trajectories. Dev Sci 10:. doi: 10.1111/j.1467-7687.2007.00595.x

Schmithorst VJ, Wilkes M, Dardzinski BJ, Holland SK (2005) Cognitive functions correlate with white matter architecture in a normal pediatric population: A diffusion tensor HRI study. Hum Brain Mapp 26:139–147. doi: 10.1002/hbm.20149

Seghier ML, Price CJ (2011) Explaining left lateralization for words in the ventral occipitotemporal cortex. J Neurosci 31:14745–53. doi: 10.1523/JNEUROSCI.2238-11.2011

Simon O, Cohen L, Bihan D Le, et al (2002) Topographical Layout of Hand , Eye , Calculation , and Language-Related Areas in the Human Parietal Lobe. 33:475–487

Smith SM, Nichols TE (2009) Threshold-free cluster enhancement: Addressing problems of smoothing, threshold dependence and localisation in cluster inference. Neuroimage 44:83–98. doi: 10.1016/j.neuroimage.2008.03.061

Stevens WD, Kravitz DJ, Peng CS, et al (2017) Privileged Functional Connectivity between the Visual Word Form Area and the Language System. J Neurosci 37:5288–5297. doi: 10.1523/JNEUROSCI.0138-17.2017

Stevens WD, Tessler MH, Peng CS, Martin A (2015) Functional connectivity constrains the category-related organization of human ventral occipitotemporal cortex. Hum Brain Mapp 36:2187–206. doi: 10.1002/hbm.22764

Stuart M, Coltheart M (1988) Does reading develop in a sequence of stages? Cognition 30:139–181. doi: 10.1016/0010-0277(88)90038-8

Takemura H, Rokem A, Winawer J, et al (2015) A Major Human White Matter Pathway Between Dorsal and Ventral Visual Cortex. Cereb Cortex 1–10. doi: 10.1093/cercor/bhv064

Thiebaut de Schotten M, Cohen L, Amemiya E, et al (2014) Learning to read improves the structure of the arcuate fasciculus. Cereb Cortex 24:989–95. doi: 10.1093/cercor/bhs383

van der Mark S, Bucher K, Maurer U, et al (2009) Children with dyslexia lack multiple specializations along the visual word-form (VWF) system. Neuroimage 47:1940–9. doi: 10.1016/j.neuroimage.2009.05.021

Vanderauwera J, De Vos A, Forkel SJ, et al (2018) Neural organization of ventral white matter tracts parallels the initial steps of reading development: A DTI tractography study. Brain Lang 183:32–40. doi: 10.1016/j.bandl.2018.05.007

Vanderauwera J, Vandermosten M, Dell'Acqua F, et al (2015) Disentangling the relation between left temporoparietal white matter and reading: A spherical deconvolution tractography study. Hum Brain Mapp 36:3273–3287. doi: 10.1002/hbm.22848

Vandermosten M, Boets B, Wouters J, Ghesquière P (2012) A qualitative and quantitative review of diffusion tensor imaging studies in reading and dyslexia. Neurosci Biobehav Rev 36:1532–52. doi: 10.1016/j.neubiorev.2012.04.002

Vidyasagar TR (1999) A neuronal model of attentional spotlight: Parietal guiding the temporal. Brain Res Rev 30:66–76. doi: 10.1016/S0165-0173(99)00005-3

Vigneau M, Beaucousin V, Hervé PY, et al (2006) Meta-analyzing left hemisphere language areas: phonology, semantics, and sentence processing. Neuroimage 30:1414–32. doi: 10.1016/j.neuroimage.2005.11.002

Vinckier F, Dehaene S, Jobert A, et al (2007) Hierarchical coding of letter strings in the ventral stream: dissecting the inner organization of the visual word-form system. Neuron 55:143–56. doi: 10.1016/j.neuron.2007.05.031

Vinckier F, Naccache L, Papeix C, et al (2006) "What" and "where" in word reading: ventral coding of written words revealed by parietal atrophy. J Cogn Neurosci 18:1998–2012. doi: 10.1162/jocn.2006.18.12.1998

Wandell B a, Yeatman JD (2013) Biological development of reading circuits. Curr Opin Neurobiol 23:261–8. doi: 10.1016/j.conb.2012.12.005

Wang Y, Gupta A, Liu Z, et al (2011) DTI registration in atlas based fiber analysis of infantile Krabbe disease. Neuroimage 55:1577–86. doi: 10.1016/j.neuroimage.2011.01.038

Weiner KS, Yeatman JD, Wandell BA (2016) The posterior arcuate fasciculus and the vertical occipital fasciculus. Cortex 10–12. doi: 10.1016/j.cortex.2016.03.012

Welcome SE, Joanisse MF (2014) Individual differences in white matter anatomy predict dissociable components of reading skill in adults. Neuroimage 96:261–275. doi: 10.1016/j.neuroimage.2014.03.069

Winkler AM, Ridgway GR, Webster MA, et al (2014) Permutation inference for the general linear model. Neuroimage 92:381–397. doi: 10.1016/j.neuroimage.2014.01.060

Yeatman JD, Dougherty RF, Ben-Shachar M, Wandell BA (2012) Development of white matter and reading skills. Proc Natl Acad Sci U S A 109:E3045-53. doi: 10.1073/pnas.1206792109

Yeatman JD, Dougherty RF, Rykhlevskaia E, et al (2011) Anatomical properties of the arcuate fasciculus predict phonological and reading skills in children. J Cogn Neurosci 23:3304–17. doi: 10.1162/jocn_a_00061

Yeatman JD, Weiner KS, Pestilli F, et al (2014) The vertical occipital fasciculus: A century of controversy resolved by in vivo measurements. Proc Natl Acad Sci 111:E5214–E5223. doi: 10.1073/pnas.1418503111

Zatorre RJ, Fields RD, Johansen-berg H (2012) Plasticity in gray and white : neuroimaging changes in brain structure during learning. Nat Publ Gr 15:528–536. doi: 10.1038/nn.3045

Zhang H, Yushkevich P a, Alexander DC, Gee JC (2006) Deformable registration of diffusion tensor MR images with explicit orientation optimization. Med Image Anal 10:764–85. doi: 10.1016/j.media.2006.06.004

Zoccolotti P, De Luca M, Di Pace E, et al (2005) Word length effect in early reading and in developmental dyslexia. Brain Lang 93:369–373. doi: 10.1016/j.bandl.2004.10.010

Tables

Table 1: Changes in DTI parameters with reading scores controlling for age.

Partial correlations are shown for changes (Δ) in DTI indices and reading scores (words/min) over the first year (TP2-TP1) and second year (TP3-TP2) of reading instruction corrected for changes in age. Pearson's r is presented together with the uncorrected p values, and values adjusted with a False Discovery Rate (FDR) correction (p_{cor}). Only the word-specific tract showed a significant correlation over the first year (*$p_{cor} \leq 0.05$): independent of age increase, RD decreases with the reading score, suggesting that learning to read affects or relies on the microstructure of the tract. See Fig. 4 for a graphical representation of these results.

	Houses r / p / p_{cor}	Faces r / p / p_{cor}	Words r / p / p_{cor}	Tools r / p / p_{cor}
TP2-TP1				
ΔFA	-0.388 / 0.302 / 0.692	-0.154 / 0.692 / 0.692	-0.329 / 0.388 / 0.692	0.187 / 0.629 / 0.692
ΔAD	0.567 / 0.112 / 0.149	0.653 / 0.056 / 0.113	-0.741 / 0.022 / 0.09	0.025 / 0.949 / 0.949
ΔRD	0.621 / 0.074 / 0.139	0.577 / 0.104 / 0.139	-0.811 / 0.008 / 0.032*	0.051 / 0.895 / 0.895
TP3-TP2				
ΔFA	0.132 / 0.777 / 0.789	0.465 / 0.293 / 0.586	0.125 / 0.789 / 0.789	0.557 / 0.194 / 0.586
ΔAD	-0.634 / 0.126 / 0.505	-0.456 / 0.303 / 0.607	-0.224 / 0.629 / 0.629	-0.248 / 0.591 / 0.629
ΔRD	-0.658 / 0.108 / 0.433	-0.454 / 0.306 / 0.6	-0.211 / 0.65 / 0.65	-0.344 / 0.45 / 0.6

Figures

Fig. 1 Reading progression as a function of age in the child cohort.

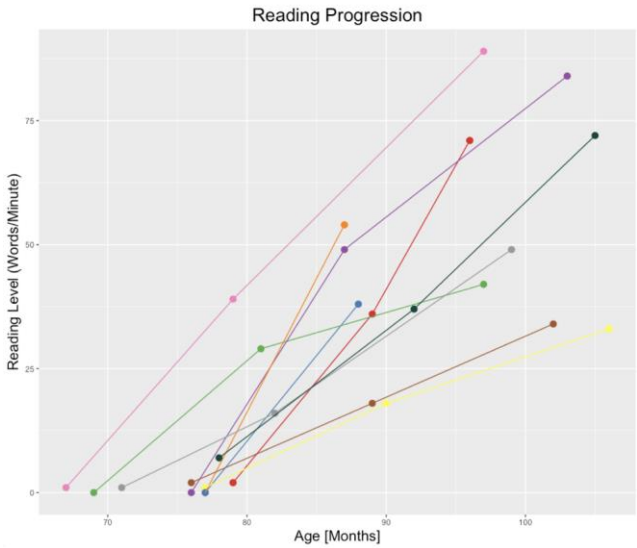

Ten children were followed throughout the first two years of reading instruction (each line represents a different child). Shown are the reading scores for the three time points where diffusion MRI data were obtained. Inter-individual differences in age relied on the differing birthday month within the calendar year, compared to the fixed time points on the scholastic calendar (September – June). While all children were poor-readers at TP1, their reading accelerated considerably over the course of the first and second years (TP2 and TP3). Note also that the variability in reading abilities across children increased with instruction, some children progressing faster than others

Fig. 2 Characterization of category-specific selection regions and tracts.

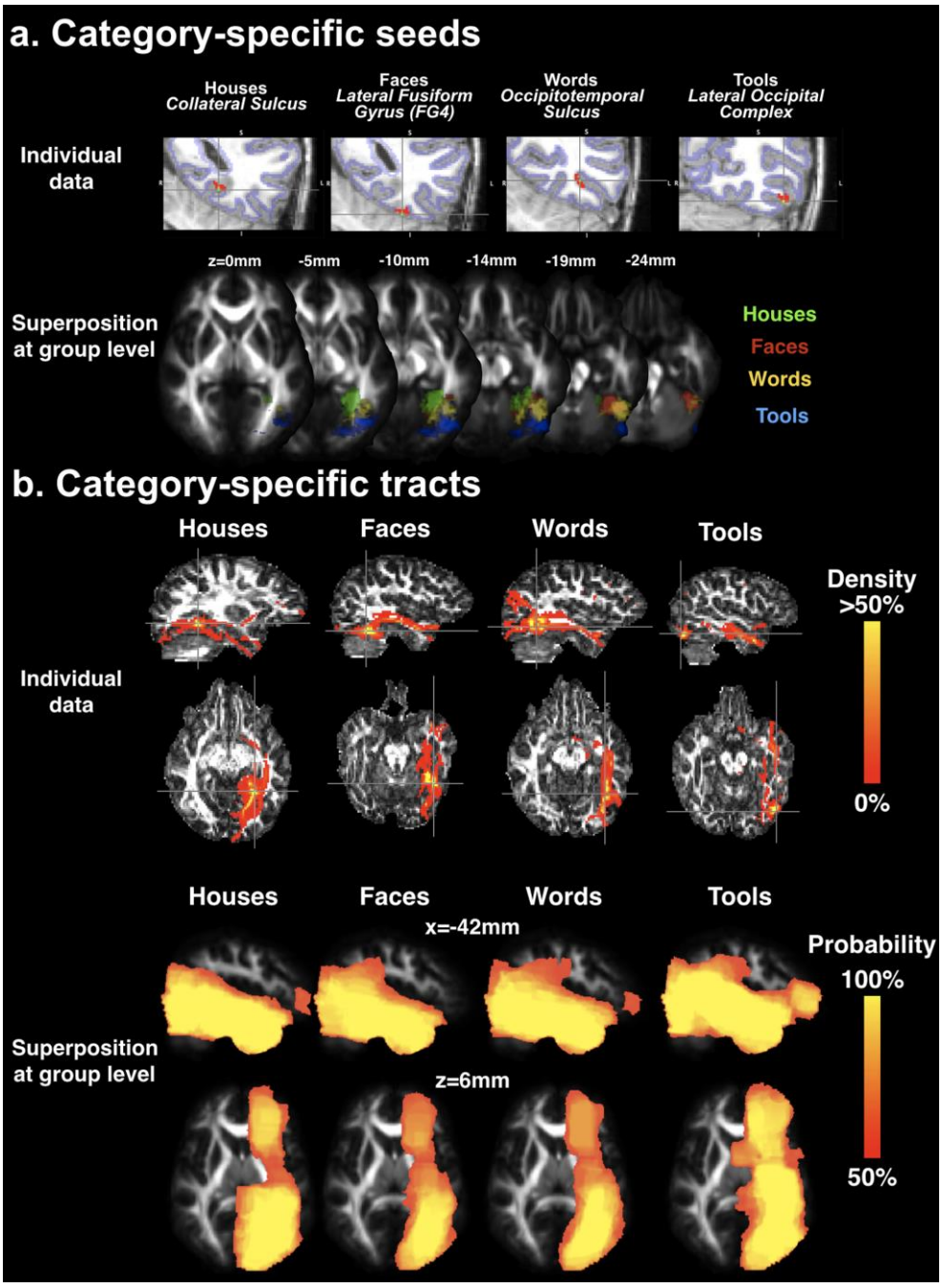

a. Selection Regions Top row: For each visual category, the selection region (in red) was identified for each subject based on functional peaks, projected, and dilated within the sub-cortical white matter segmentation (shown in purple on T1w images). Visual categories are presented from the more medial to the more lateral representations (from the house to tool processing regions). Bottom row: The repartition of locations of the selection regions over the children group is presented on selected axial slices of the subject-specific FA template in MNI space. Each patch of sub-cortical white matter is clearly attributed to a single functional selection region.

b. Category-specific tracts Top rows: The density maps of streamlines were computed for each subject and each visual category (same subject as in part a). Color bar represents the percentage of the maximal streamline number passing through a voxel. Bottom rows: Tract probability maps were computed over the group by normalizing and averaging the binarized and smoothed individual density maps. Regions of at least 50% overlap over our children cohort are shown on a sagittal and axial slice in MNI space.

Fig. 3 Specific connectivity of the visual category processing regions.

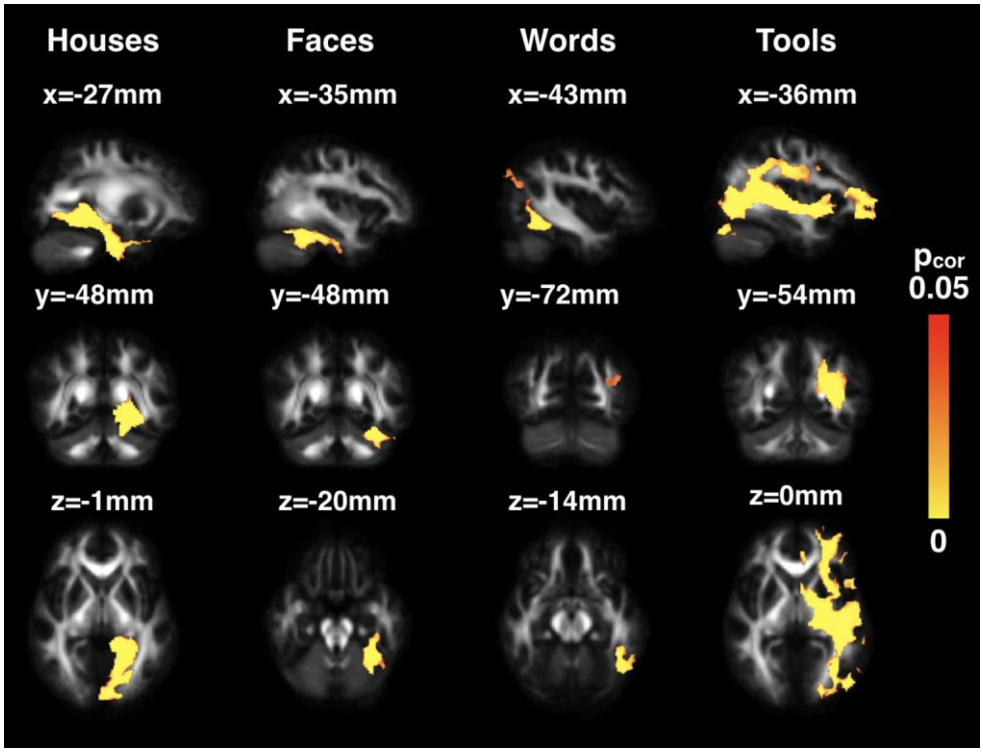

For each category, statistical analyses showed the connectivity clusters with different location compared with other categories. Color bar represents the FWE-corrected p-value (p_{cor}). Slice coordinates are given in MNI space.

Fig. 4 Tract-specific microstructural changes over the first year of reading instruction.

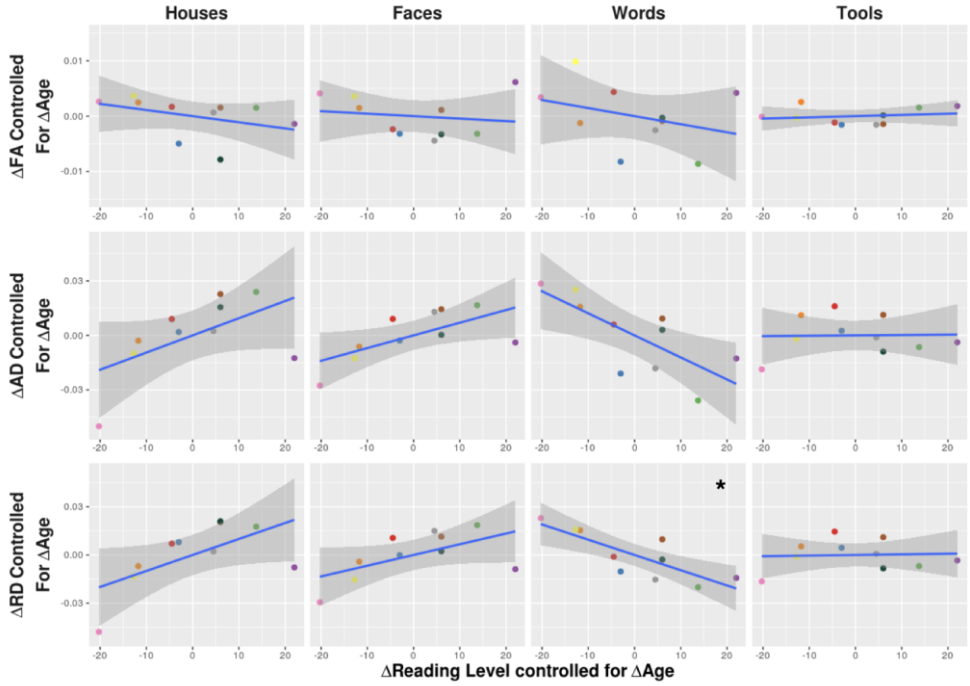

Improvements in reading level (words/minute) between the beginning and the end of the first school year of reading instruction (Δ = TP2-TP1) were compared to changes in fractional anisotropy (FA), axial diffusivity (AD), and radial diffusivity (RD) within the specific connectivity clusters of each visual category (Fig. 3) after controlling for age increase. Only the word-specific tract showed a significant correlation between RD and reading improvement (*p_{cor}<0.05, False Discovery Rate corrected), suggesting that this learning relies and/or induces specific microstructural changes within the connections dedicated to this cognitive process. Best-fit lines with 95% confidence intervals are shown. Each subject is represented by the same color dot as in Fig. 1

Supplementary Methods

Information relevant to functional MRI aspects of the study, from [Dehaene-Lambertz et al., 2018].

Dehaene-Lambertz G, Monzalvo K, Dehaene S (2018): The emergence of the visual word form: Longitudinal evolution of category-specific ventral visual areas during reading acquisition. Ed. Kalanit Grill-Spector. PLOS Biol 16:e2004103.

Image acquisition and paradigm for functional data

Anatomical images were obtained with a magnetization prepared radio frequency pulses and rapid gradient echo (MPRAGE) sequence with a resolution of $1x1x1mm^3$, echo time (TE) of 4.18ms, repetition time (TR) of 2300ms, and inversion time (TI) of 900ms. Functional images were obtained with an EPI echo gradient sequence with TE=30ms, and TR=2400ms and isotropic $3mm^3$ voxels.

For the fMRI paradigm, subjects were presented with stimuli belonging to the categories of houses, faces, words, numbers, tools, bodies and high-frequency and low-frequency grids with variable orientations. Here, we focused on the runs for houses, faces, words, and tools since we aimed to describe the visual mosaic around the word category in the vOTC. Each category comprised 60 different exemplars, either using black-and-white pictures for houses, tools, and faces or four-character strings for words. The words were frequent and regular words. Faces were front views of male and female children faces. Tools were pictures of objects frequently encountered in a child's daily life (scissors, spoons, shoes, etc.). Six subsets comprising 10 exemplars of each category were created, to be successively used in the six scanning sessions. The order of the subsets was different for each child.

We used a mini-block design. Blocks of six images belonging to the same category were randomly selected and presented during 1s each, thus forming a 6-second block. Blocks were separated by a variable inter-block interval of 2.4, 3.6 or 4.8 s (mean of 3.6 s). Thus, a new series of images was presented on average every 9.6 s. The order of the categories was randomly chosen, with the constraint that each category be presented three times in a functional run (8 categories x 3 repetitions = 24 blocks of 6 images each). Within each block, a target (the picture of the cartoon character "Waldo") has a 33% chance to appear, replacing one of the six images (excluding the first two images of the block). Thus, an average of 8 targets appeared during a run of 24 blocks. Children were instructed to press a button as soon as they detected Waldo. This task was used to keep the child's attention focused toward the visual stimuli. The total run duration was 3min 58s. In each fMRI session, 4 runs were acquired, except for the first and 6^{th} sessions in which only 3 runs were acquired due to the additional tests and sequences (e.g. diffusion MRI) proposed to the children in these sessions. In the 7^{th} session (N=8), 4 runs were acquired except for two children who asked to stop the acquisition after the third run.

A training in a mock scanner was used before the first MRI session to familiarize children with the scanner environment, then children were brought to the 3T MRI scanner (Siemens Trio). They were protected with noise-protection ear-phones and a mirror system above their head allowed them to see the visual stimuli presented on a screen at the end of the tunnel. The images were projected onto this screen subtending 42.5 cm width and viewed through a mirror from a distance of 125 cm, for an overall angular size of 19.3 degrees. Stimulus presentation and behavioral responses collection were performed using PsychToolbox, a free Matlab toolbox (MathWorks, USA). To reduce head motion, the quality of the MRI images was checked after each sequence acquisition and verbal feedback was given to the child.

Preprocessing of functional images

To correct for motion within each run, images were first realigned using the corresponding tool provided by SPM8 (http://www.fil.ion.ucl.ac.uk/spm/), including both estimation and reslicing steps. The target image was the mean of all images, except if movement during acquisition corrupted the mean image. In that case, the first image was used. Average movement amounted to a few millimeters in translation and a fraction of a degree. Each fMRI volume was then visually inspected one by one. Using the Matlab toolbox ArtRepair (http://cibsr.stanford.edu/tools/human-brain-project/artrepair-software.html), images affected by excessive intravolume movement artifacts (stripes, severe shape or size distortion) were replaced by linear interpolation of previous and subsequent images, or by nearest-

neighbor interpolation when the damaged volume was the first or the last or when several consecutive images were affected. The percentage of rejected images remained low, with the majority of sessions requiring no correction at all (65% of fMRI sessions). The mean rejection percentage across the 68 sessions was 0.77% (standard deviation = 1.1%; range 0-16%).

Corrected images were then ready to undergo the rest of the preprocessing, i.e. slice timing, coregistration to the anatomy acquired on the same session, and normalization. For normalization, the T1-weighted anatomical images were first normalized to the standard European adult MNI template. This step segmented the images automatically into different tissue classes (grey matter, white matter, and nonbrain, i.e. cerebrospinal fluid and skull), using the "New Segmentation" option in SPM8. By averaging those segmented images across all 10 subjects and all 7 sessions, three tissue probability maps were obtained to create a new target template. The original T1 images were then normalized a second time, this time using as the target template. The highly accurate alignment of the 6 or 7 anatomical images obtained from the same child was verified using the CheckReg tool in SPM8. Finally, the normalization matrix was applied to all EPI images of the corresponding session, with a final resampled voxel size of 2x2x2 mm.

Supplementary Table 1: Subject characteristics

The age and reading scores are presented for each child at the beginning, end of the first year of reading instruction, and one year later, together with the sex (M = male, F = female) and handedness (R = right-handed, L = left-handed). Mean and standard deviations (SD) over the group are also presented.

			Beginning of School Year (TP1)		End of School Year (TP2)		End of Following School Year (TP3)	
Subject	Sex	Handedness	Age (Months)	Words/Min	Age (Months)	Words/Min	Age (Months)	Words/Min
1	F	R	67	1	79	39	97	89
2	F	R	69	0	81	29	97	42
3	M	R	71	1	82	16	99	49
4	F	R	75	0	87	54		
5	M	L	76	0	87	49	103	84
6	F	R	76	2	89	18	102	34
7	F	R	76	0	88	38		
8	M	R	77	1	90	18	106	33
9	M	R	78	7	92	37	105	72
10	M	R	79	2	89	36	96	71
Mean			74.4	1.4	86.4	33.4	100.6	59.3
SD			4.0	2.1	4.3	13.1	3.9	22.4

Supplementary Table 2: Peak coordinates of visual categories in MNI-space (mm).

T statistics are given for the peak voxel of each cluster.

	Houses		Faces		Words		Tools	
Subject	x,y,z (mm)	T	x,y,z (mm)	T	x,y,z (mm)	T	x,y,z (mm)	T
1	-28,-48,-10	10.9	-38,-52,-22	11.0	-40,-56,-6	5.5	-48,-70,-14	11.8
2	-32,-50,-10	3.2	-38,-52,-18	7.7	-40,-58,-16	2.4	-44,-68,-12	8.0
3	-28,-50,-6	9.5	-38,-52,-18	18.7	-40,-56,-6	9.1	-48,-76,-14	10.2
4	-26,-52,-4	6.6	-38,-56,-22	17.1	-48,-54,-18	5.6	-42,-72,-16	9.3
5	-30,-48,-4	6.5	-34,-50,-22	11.0	-44,-54,-20	6.3	-40,-64,-8	11.2
6	-24,-50,-10	6.5	-30,-53,-22	16.2	-32,-62,-16	5.2	-24,-74,-6	6.7
7	-30,-48,-4	6.5	-32,-56,-12	8.8	-48,-58,-18	4.4	-38,-64,-10	6.9
8	-36,-44,-10	5.6	-34,-48,-24	6.6	-40,-66,-12	5.6	-44,-70,-8	11.6
9	-32,-52,-8	6.3	-38,-50,-24	14.3	-50,-60,-12	4.9	-46,-68,-4	5.7
10	-32,-56,-8	8.5	-38,-58,-22	6.2	-50,-56,-16	7.1	-36,-72,-6	7.7
Mean	-29.8,-49.8,-7.4		-36.2,-53.0,-20.6		-43.2,-58.0,-14.0		-41.0,-69.8,-9.8	
SD	3.5,3.2,2.7		3.6,3.2,3.7		5.8,3.8,4.9		7.2,3.9,4.0	

Using paired t-tests, we compared the location of functional peaks of adjacent visual categories (i.e., houses-faces and words vs. tools) along the lateral-medial axis (i.e., x-coordinates in MNI-space). We found that the house peaks were located significantly more medially than the face peaks ($\Delta x_{houses-faces}$=+6.0 ± 4.1mm, p=0.001), whereas there was more overlap between the word and tool peaks along this axis ($\Delta x_{words-tools}$= -2.2 ± 7.7mm, p=0.4). Moreover, the distance between the house and face peaks was significantly larger than the distance between word and tool peaks ($\Delta x_{houses-faces} - \Delta x_{words-tools}$ = 8.2 ± 8.2mm, p=0.01). Since the words and tool peaks were at similar x-coordinates and both tracts travel in the antero-posterior direction, there was likely more overlap in these tracts than for the house vs face tracts. Therefore, removing the tool connectivity likely yielded more differences for the word connectivity than the house connectivity did for the face connectivity (see Supplementary Figure 2).

Supplementary Table 3: Paired t-tests for longitudinal changes in DTI parameters

Presented are the paired t-tests of the DTI parameters in the specific connectivity cluster of each visual category from TP1 to TP2 (top table), and from TP2 to TP3 (bottom table). The mean and standard deviation (SD) of changes are given below, as well as the t statistics, uncorrected p-values, and False Discovery Rate corrected p-values (p_{cor}) (*$p_{cor} \leq 0.05$).

TP2-TP1	Houses Mean ± SD t / p / p_{cor}	Faces Mean ± SD t / p / p_{cor}	Words Mean ± SD t / p / p_{cor}	Tools Mean ± SD t / p / p_{cor}
FA	-0.0013 ± 0.0038 -1.066 / 0.314 / 0.419	0.0038 ± 0.0045 2.654 / 0.026 / 0.105	-0.0012 ± 0.0059 -0.623 / 0.549 / 0.549	0.0008 ± 0.0020 1.284 / 0.231 / 0.419
AD	-0.0072 ± 0.0229 -0.989 / 0.349 / 0.465	-0.0024 ± 0.0142 -0.537 / 0.604 / 0.604	-0.0085 ± 0.0222 -1.211 / 0.257 / 0.465	-0.0084 ± 0.0107 -2.503 / 0.034 / 0.135
RD	-0.0063 ± 0.0225 -0.888 / 0.397 / 0.397	-0.0071 ± 0.0160 -1.398 / 0.196 / 0.337	-0.0065 ± 0.0168 -1.223 / 0.252 / 0.337	-0.0096 ± 0.0094 -3.230 / 0.010 / 0.041*

TP3-TP2	Houses Mean ± SD t / p / p_{cor}	Faces Mean ± SD t / p / p_{cor}	Words Mean ± SD t / p / p_{cor}	Tools Mean ± SD t / p / p_{cor}
FA	0.0025 ± 0.0015 4.576 / 0.003 / 0.005*	0.0051 ± 0.0053 2.758 / 0.028 / 0.038*	0.0027 ± 0.0050 1.557 / 0.163 / 0.163	0.0049 ± 0.0030 4.710 / 0.002 / 0.005*
AD	-0.0116 ± 0.0172 -1.903 / 0.099 / 0.136	-0.0108 ± 0.0163 -1.879 / 0.102 / 0.136	0.0052 ± 0.0309 0.477 / 0.648 / 0.648	-0.0095 ± 0.0099 -2.716 / 0.030 / 0.120
RD	-0.0115 ± 0.0159 -2.037 / 0.081 / 0.108	-0.0139 ± 0.0185 -2.118 / 0.072 / 0.108	0.0025 ± 0.0284 0.249 / 0.811 / 0.811	-0.0119 ± 0.0102 -3.317 / 0.013 / 0.051

Supplementary Table 4: Correlation analysis performed with the global connectivity of each visual category.

Partial correlations are shown for changes (Δ) in DTI indices and reading scores (words/min) over the first year (TP2-TP1) and second year (TP3-TP2) of reading instruction corrected for changes in age. Pearson's r is presented together with the uncorrected p values, and values adjusted with a False Discovery Rate (FDR) correction (p_{cor}). The maps of global connectivity are presented in Supplementary Figure 1. No changes in diffusion parameters in these global maps were able to reflect reading-related improvements (all p_{cor}>0.29)

	Houses r / p / pcor	Faces r / p / pcor	Words r / p / pcor	Tools r / p / pcor
TP2-TP1				
ΔFA	0.132 / 0.735 / 0.924	0.412 / 0.271 / 0.712	0.356 / 0.347 / 0.712	0.350 / 0.356 / 0.712
ΔAD	0.355 / 0.349 / 0.712	0.358 / 0.344 / 0.712	0.163 / 0.675 / 0.924	0.040 / 0.919 / 0.924
ΔRD	0.382 / 0.310 / 0.712	0.283 / 0.460 / 0.789	0.114 / 0.771 / 0.924	0.037 / 0.924 / 0.924
TP3-TP2				
ΔFA	0.292 / 0.525 / 0.525	0.393 / 0.383 / 0.460	0.364 / 0.422 / 0.461	0.436 / 0.328 / 0.438
ΔAD	-0.712 / 0.073 / 0.298	-0.607 / 0.148 / 0.298	-0.606 / 0.149 / 0.298	-0.464 / 0.294 / 0.438
ΔRD	-0.766 / 0.044 / 0.298	-0.663 / 0.105 / 0.298	-0.64 / 0.121 / 0.298	-0.535 / 0.216 / 0.37

Supplementary Figure 1: Probability maps for the connectivity of visual categories and well-known fiber tracts

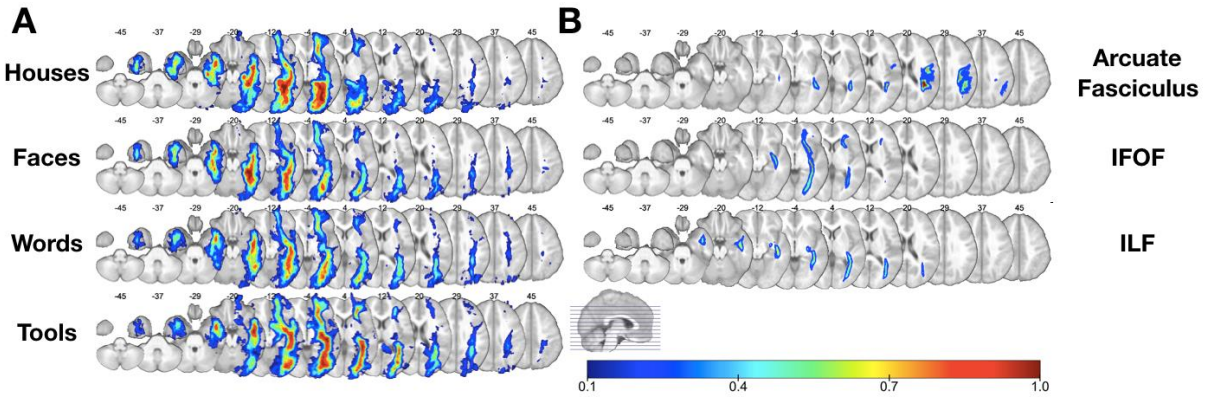

(A) Group probability maps for the connectivity of the studied visual categories and (B) probability maps for the arcuate fasciculus, inferior fronto-occipital fasiculus (IFOF), and the inferior longitudinal fasciculus (ILF) as provided by Catani et al. 2008. Axial slice coordinates are in MNI space. The color bar shows the probability for our group cohort and that used in the atlas of Catani et al. 2008.

Supplementary Figure 2: Voxel-based repeated measure ANOVA including only the face- and word-specific tracts

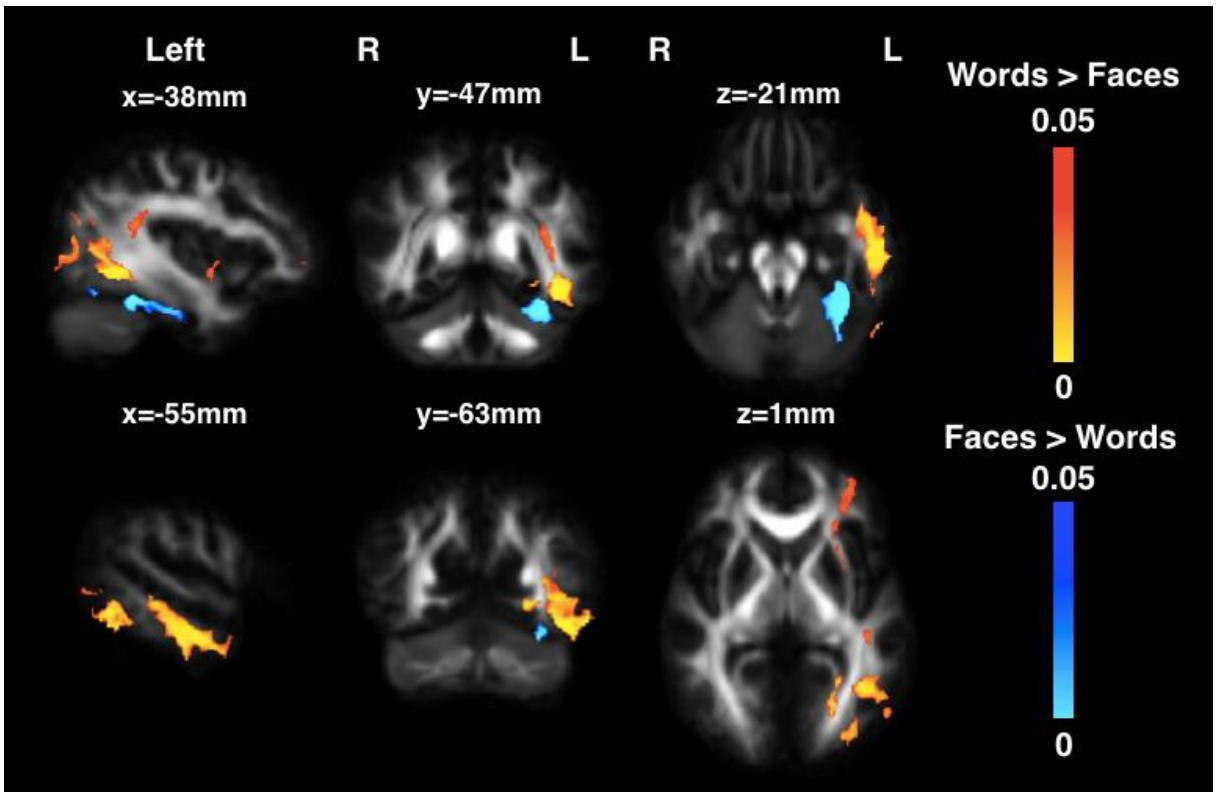

Significant specific clusters for the word (red-yellow) vs face (blue-light blue) connectivity are shown. Color bars represent the Family-Wise Error corrected p-values. Selected slices (coordinates in MNI space) highlight the most important differences. L=Left, R=Right Hemisphere.